



## 05: Mechanical properties of nanostructures

January 27, 2010

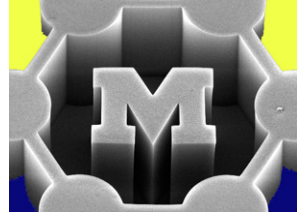
**John Hart**

[ajohnh@umich.edu](mailto:ajohnh@umich.edu)

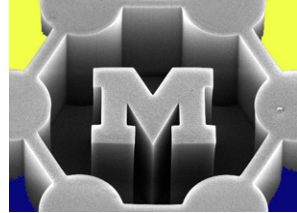
<http://www.umich.edu/~ajohnh>

# Announcements

- Mostafa's office hours Th 4.30-6.30, 1363 GGB
- PS1 questions
  - QDs close together
  - Effective mass
  - Others?



# Recap: electronic structure at the nanoscale



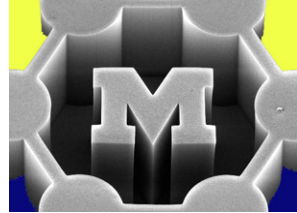
- Sensitivity of bandgap to size governs optical emission of semiconductor nanocrystals
  - $\uparrow$  size =  $\downarrow$  bandgap =  $\uparrow$  primary absorption wavelength
  - Strong confinement: can neglect e/h coupling
  - These are good yet imperfect approximations
- Dispersion relation (energy versus wavevector) gives the band structure, which determines the allowable energy levels in a material
- Probability of finding an electron (energy carrier) in a particular state is determined by a statistical distribution
- Examples (quantum size effects):
  - Single electron transistor: field modulation of band structure of a quantum dot, so discrete  $N$ 's of electrons are held at a time.
  - CNT “wrapping” condition (in reciprocal space) classifies it as a metal or semiconductor.

# Today's agenda

- What determines stiffness and strength of a material?
- Mechanical properties of 1D nanostructures: unique behavior and characterization methods
- Statistics of defects in small volumes
- Controlling bulk material strength by engineering nanoscale boundaries
- Strong materials in nature



# Today's readings (ctools)



## Nominal: (on ctools)

- Kaplan-Ashiri et al., “On the mechanical behavior of  $WS_2$  nanotubes under axial tension and compression”
- Wu et al., “Mechanical properties of ultrahigh-strength gold nanowires”

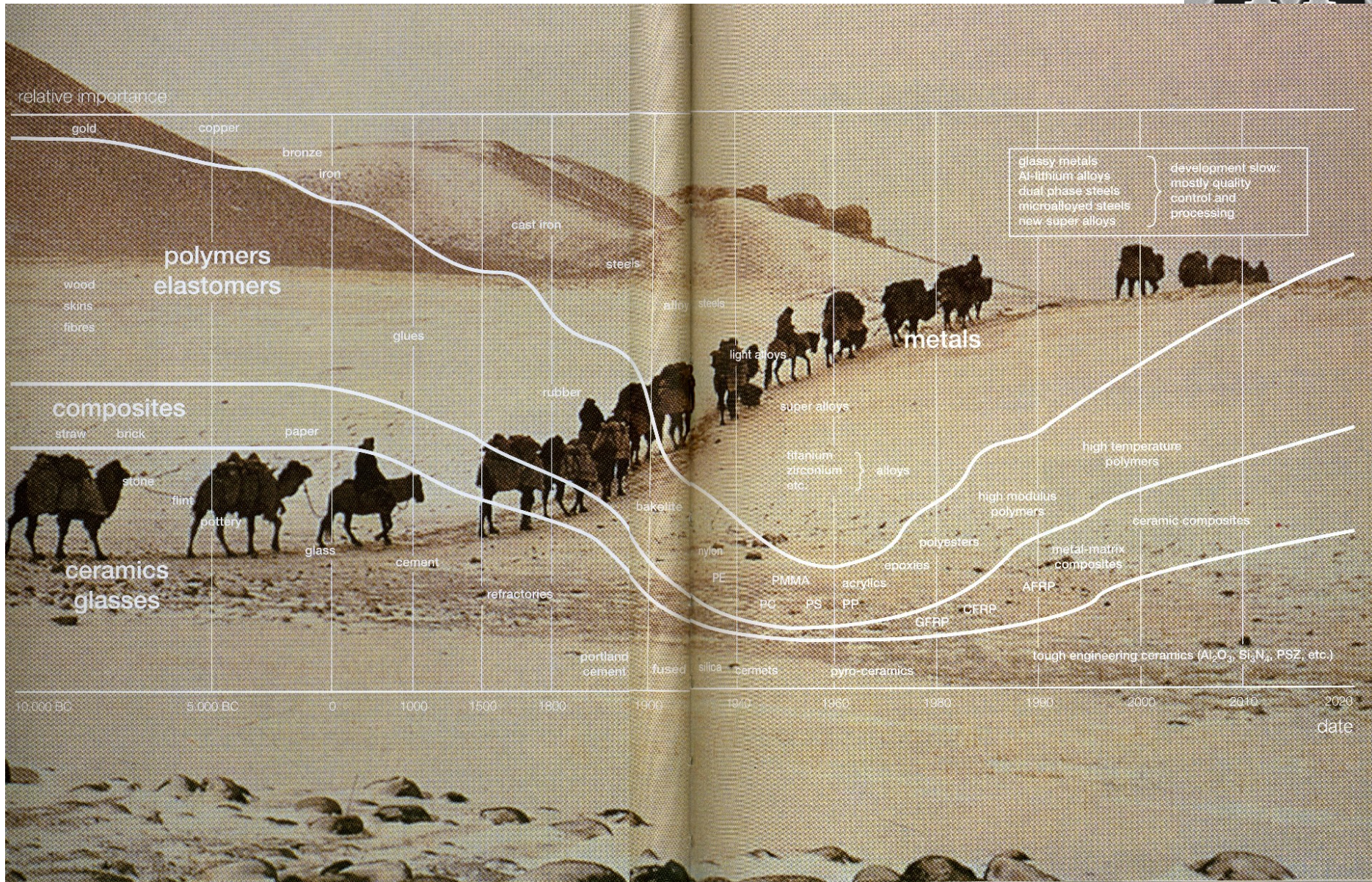
## Extras: (on ctools)

- Lu et al., “Strengthening materials by engineering coherent internal boundaries at the nanoscale”
- Trelewicz and Shih, “The Hall-Petch breakdown in nanocrystalline metals”

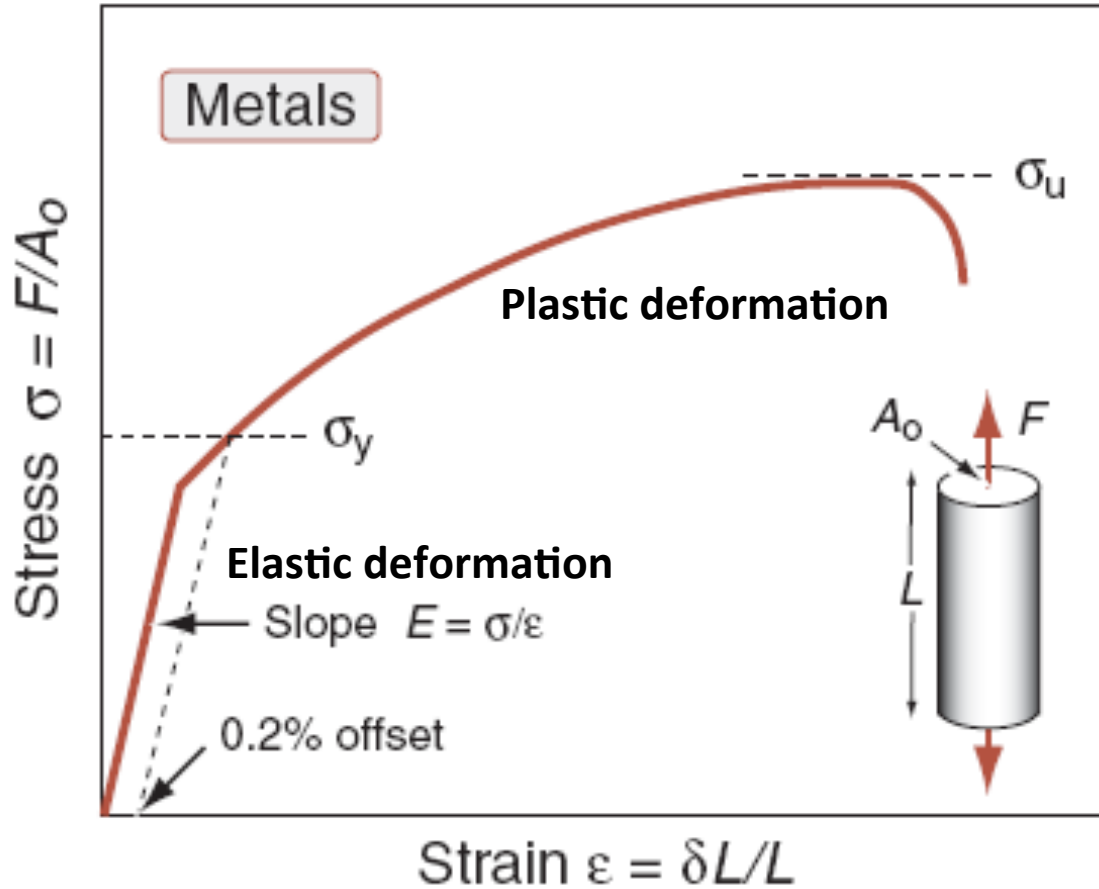
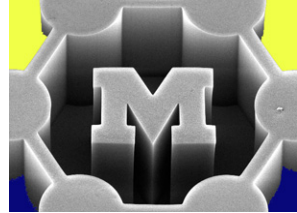
## For fun: (on ctools)

- Gao et al., “Materials become insensitive to flaws at nanoscale: Lessons from nature”
- Jensen et al., “Nanotube radio”

# From natural to engineered materials

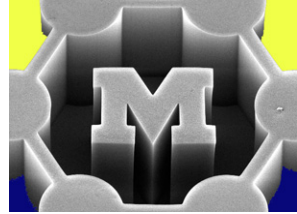


# Basic solid mechanics



## Ductile vs. brittle

# Stress and strain



- Engineering stress  $[\text{N/m}^2] = [\text{Pa}]$

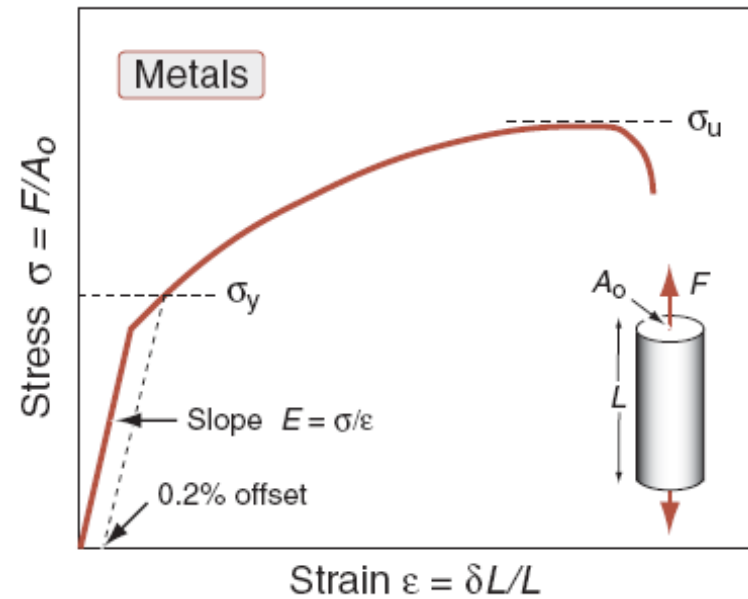
$$\sigma = \frac{P}{A_0}$$

- $A_0$  = cross sectional area **before** loading

- Engineering tensile strain

$$\varepsilon = \frac{l - l_0}{l_0}$$

- $l_0$  = length **before** loading



# Elastic deformation and yield



In the elastic region, a material will return to its original length if unloaded

- Obeys Hooke's law (linear)

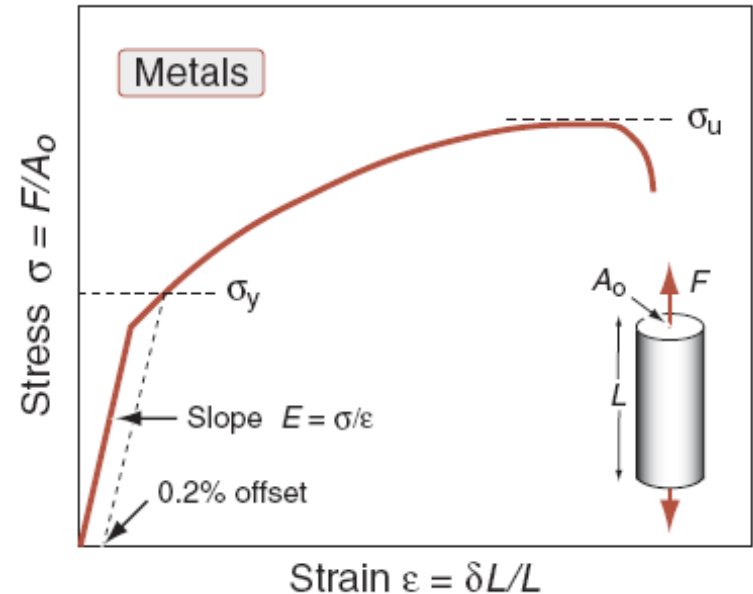
$$\sigma = E \varepsilon_t \quad E = \frac{\sigma}{\varepsilon_t}$$

- $E$ : elastic (Young's) modulus [GPa]

- Yield strength (definition)

$$\sigma_y = \frac{F_{0.0002}}{A_0} \quad \leftarrow \text{load @0.2\% permanent deformation}$$

Experimentally obtain yield strength by drawing a line parallel to elastic loading line at  $\varepsilon = 0.002$



# Plastic deformation and failure

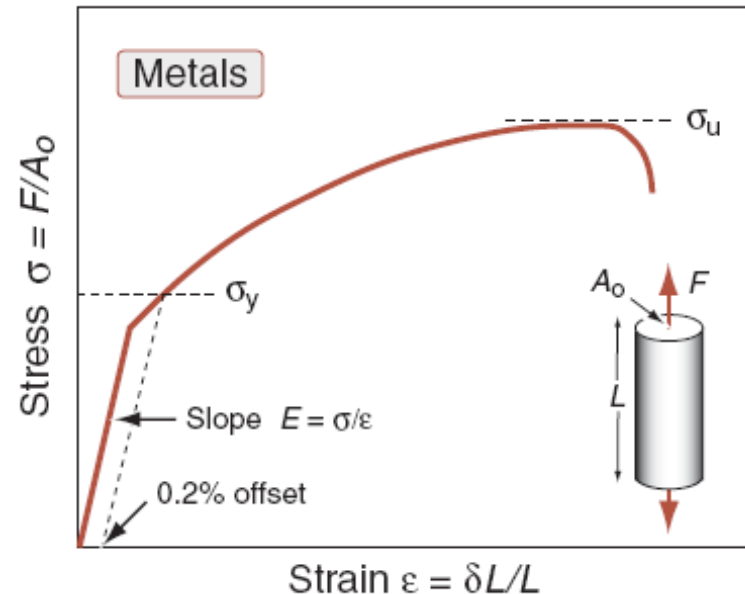


Will not return to original length if unloaded after plastic deformation occurs

- (Ultimate) tensile strength

$$\sigma_u = \frac{F_{\max}}{A_0}$$

- Recall difference between ductile and brittle materials



# Types of loading

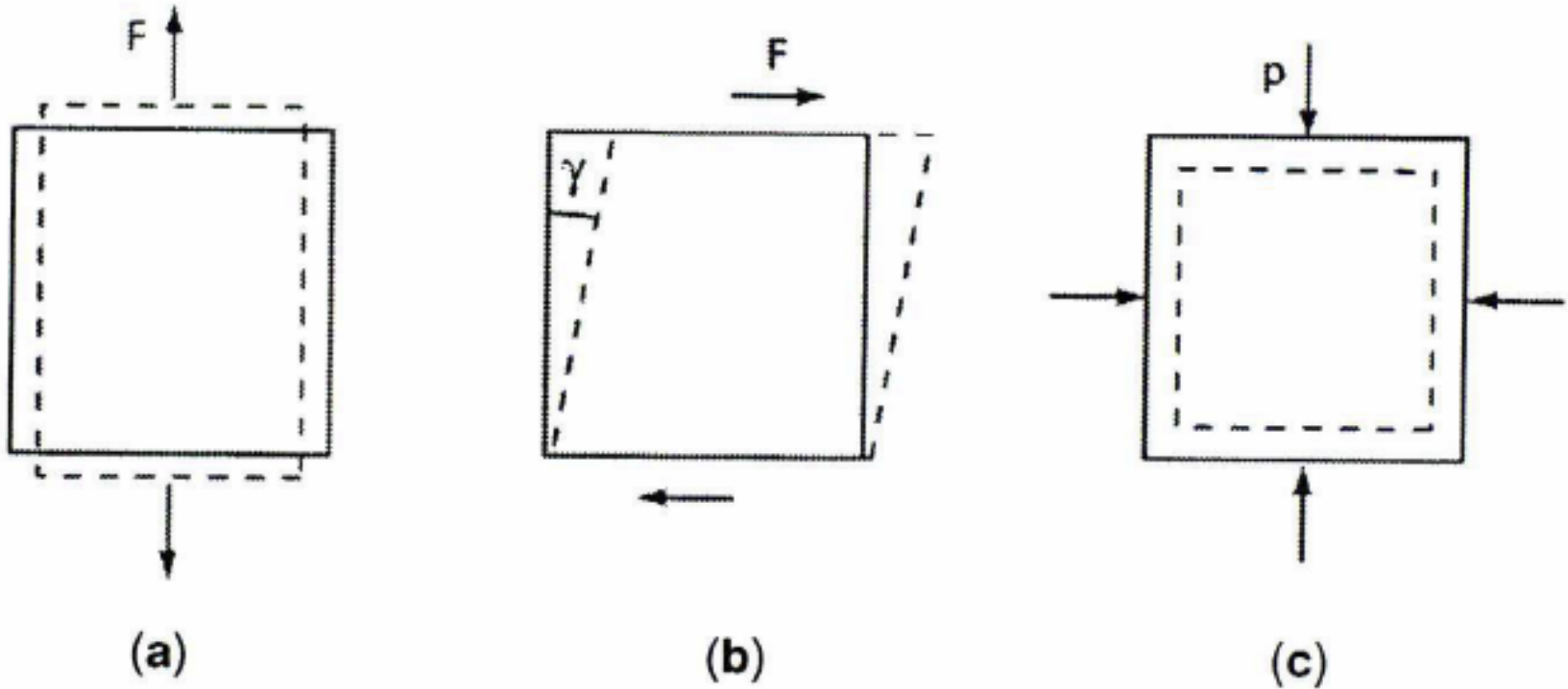
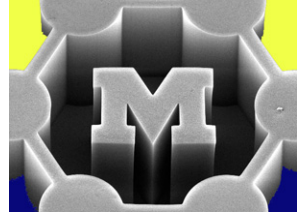


Fig. 7.1. (a) tensile test, (b) shear test, (c) hydrostatic compression



**What determines**

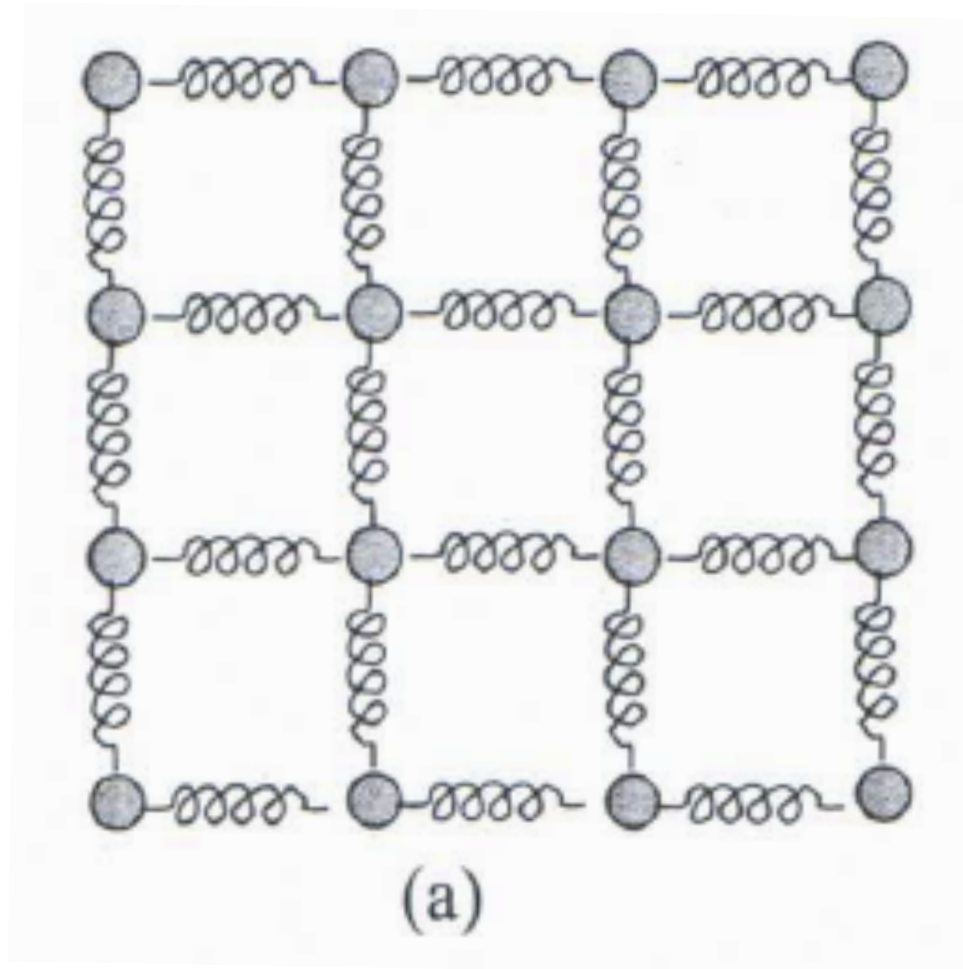
- stiffness?**
- strength?**

**Why are ceramics stiffer than polymers?**

**Why are metals more ductile than ceramics?**

**What is the ideal strength of a crystal?**

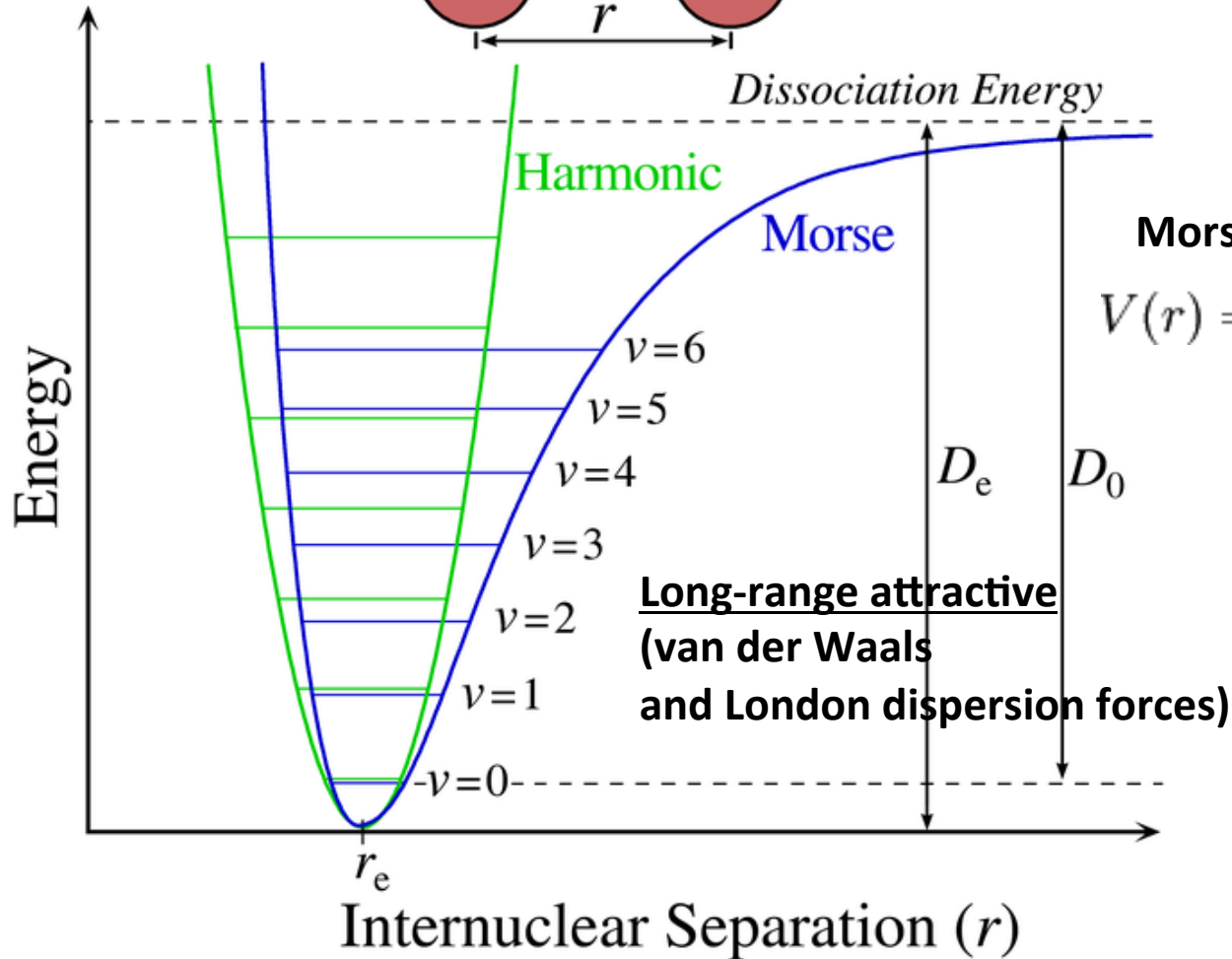
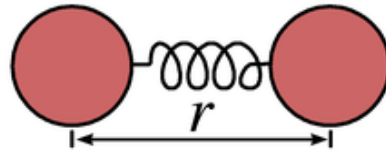
# A simple model



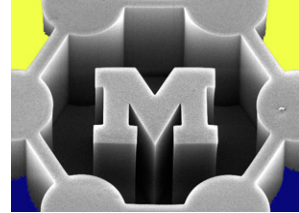
# Interatomic potential: a bond as a spring



Short-range repulsive  
(electron orbital overlap)

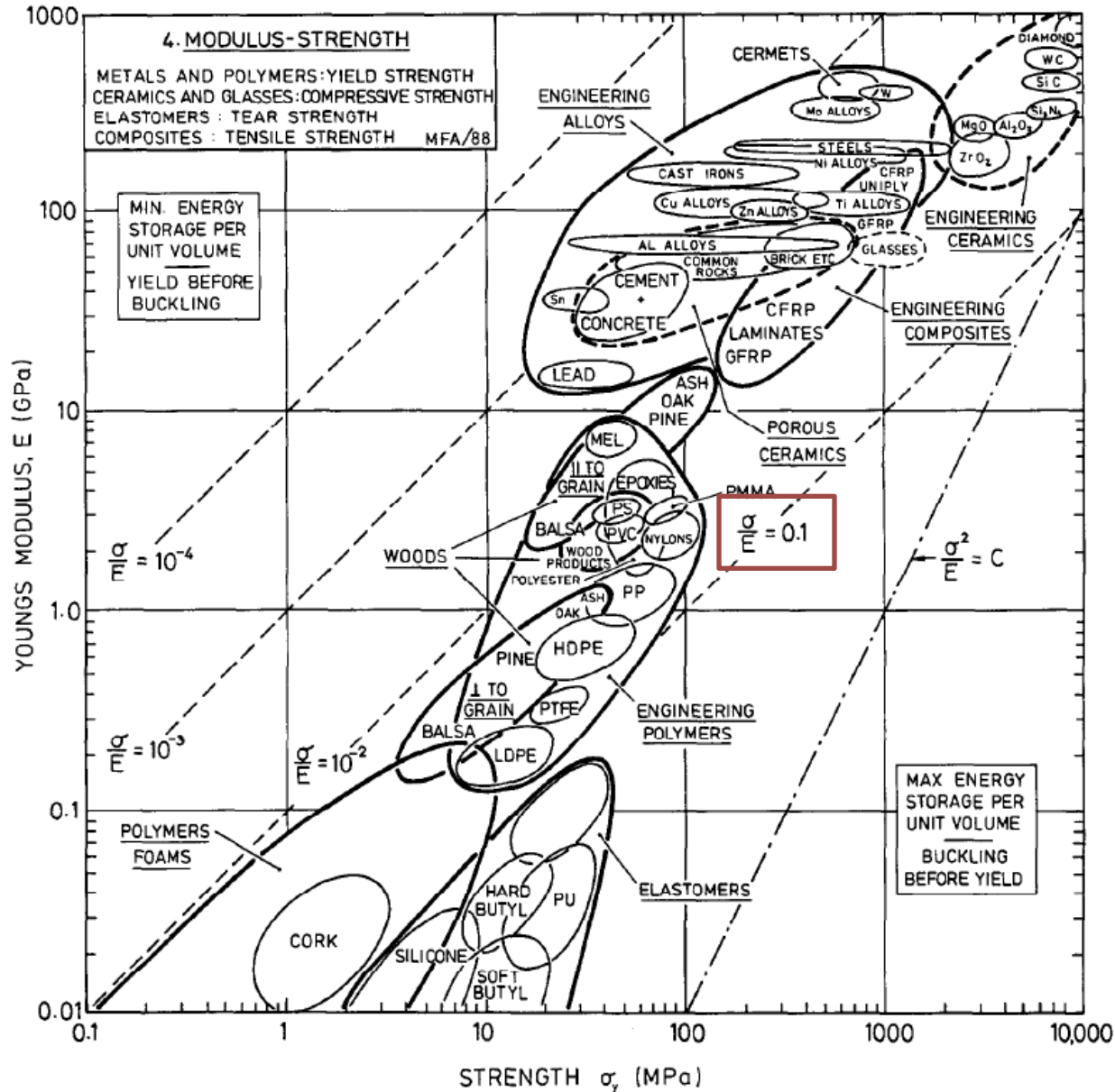


# Comparison ("Ashby" chart)

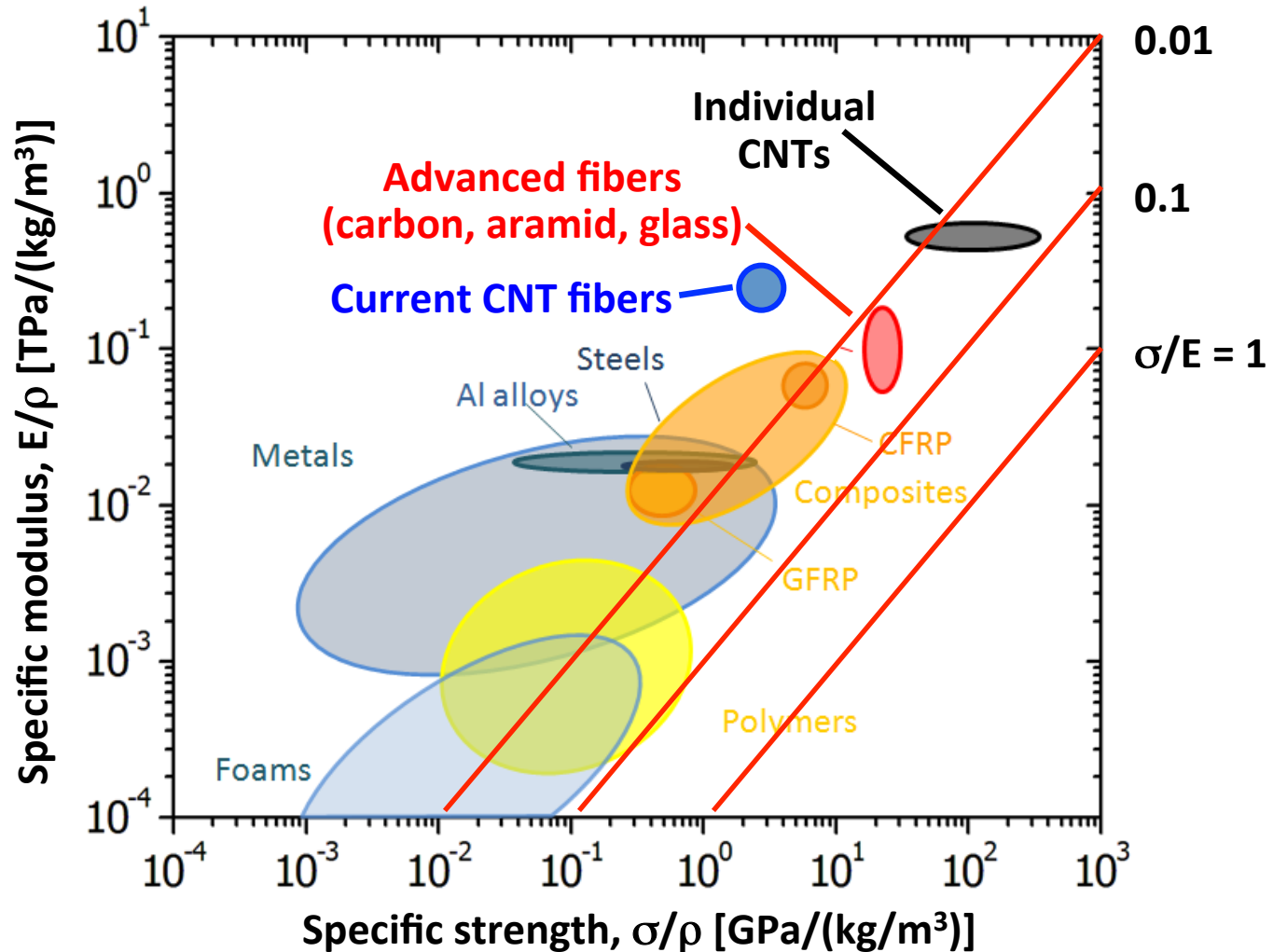
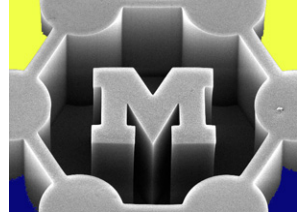


1282

ASHBY: OVERVIEW NO. 80



# Comparison



# Measuring stiffness by thermal vibration

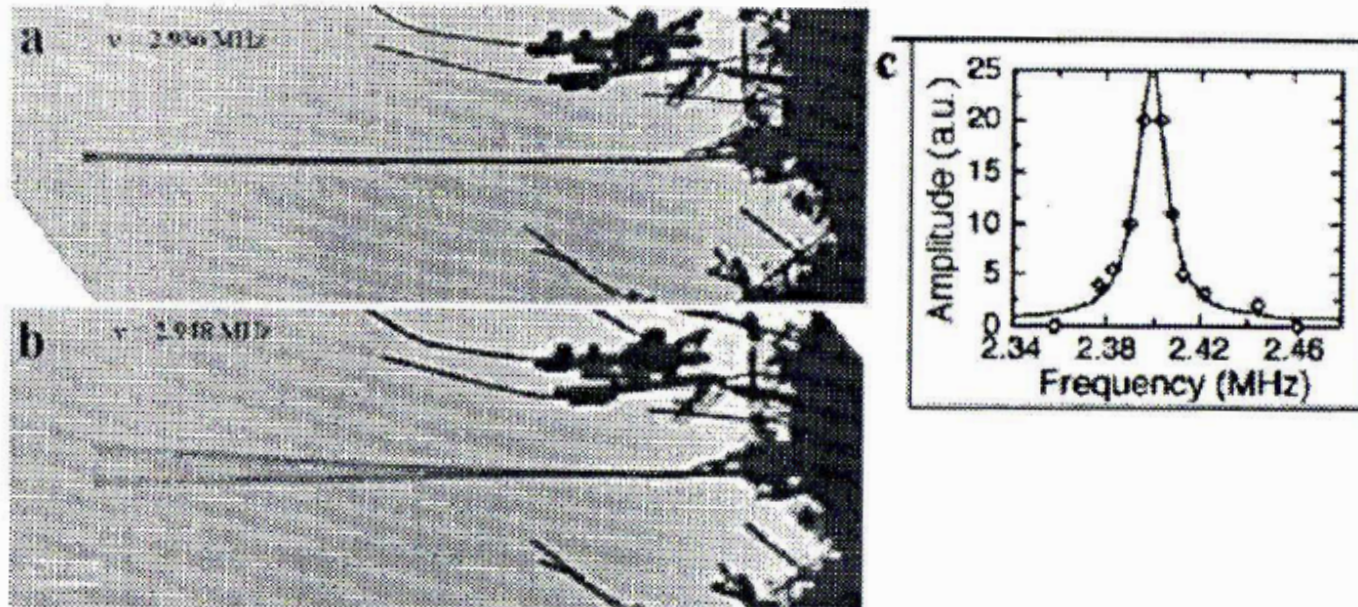
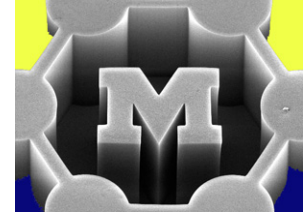
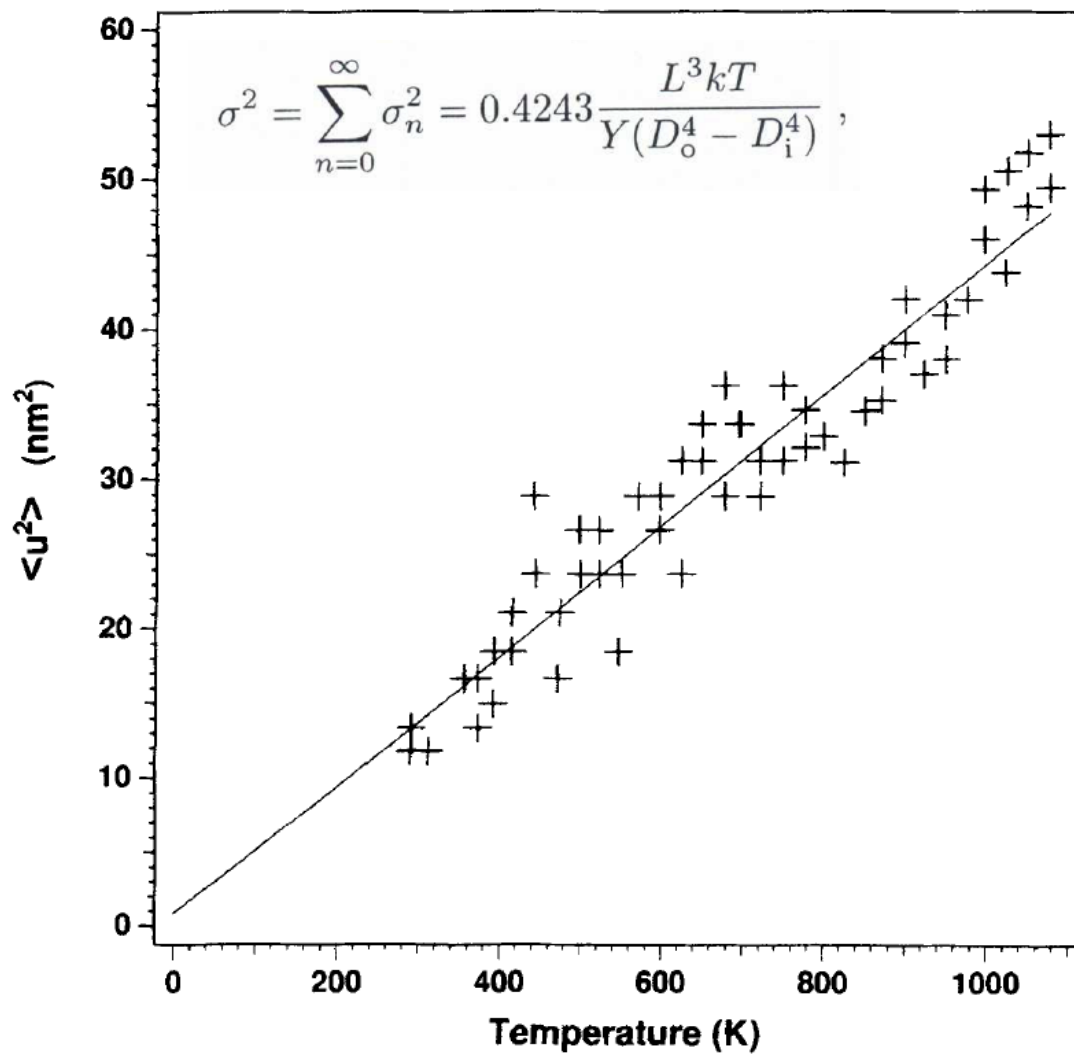
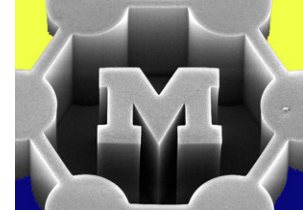
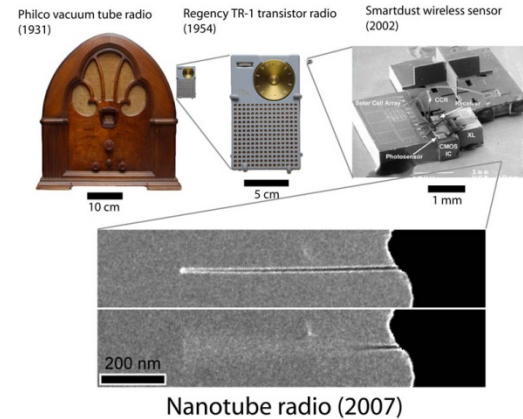
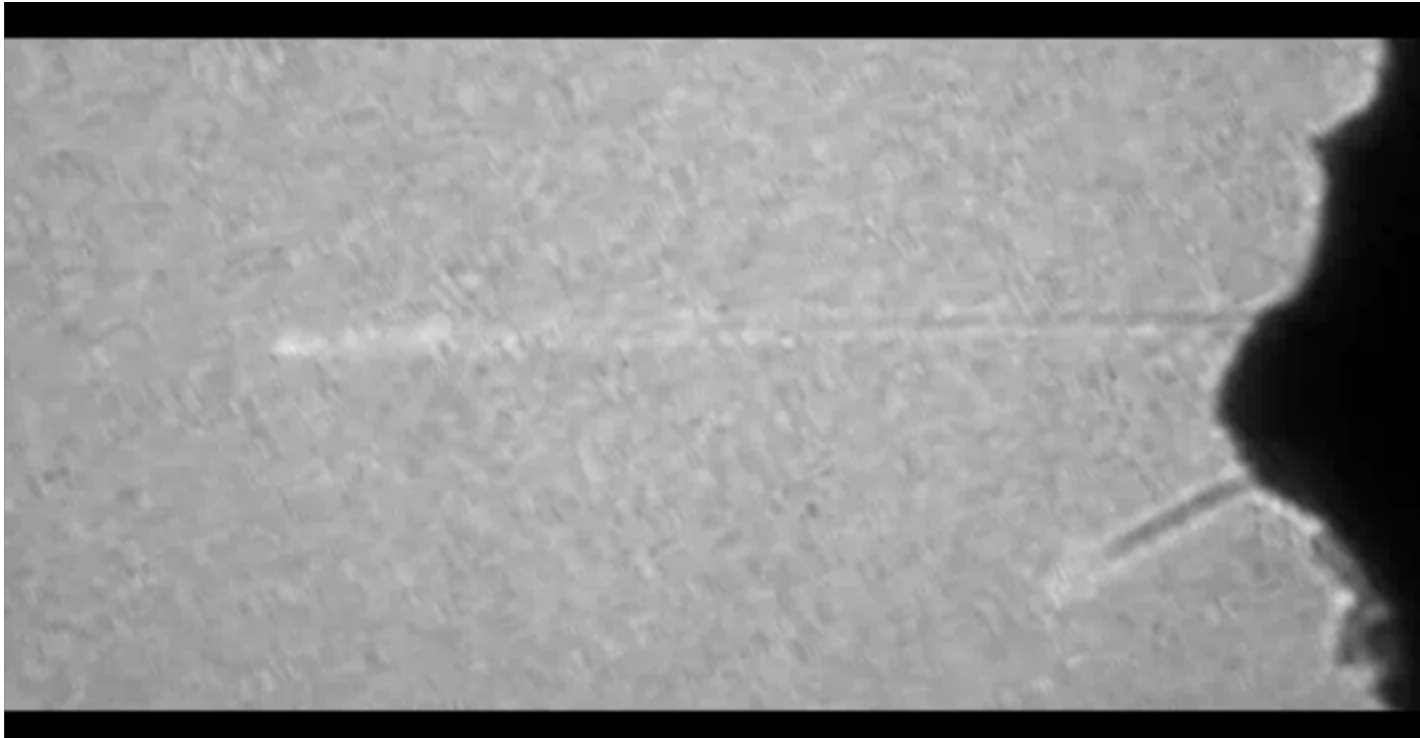


Fig. 7.10. A carbon nanotube at (a) off-resonance and (b) on-resonance. (c) The resonance peak. Reproduced from Wang et al. [73]



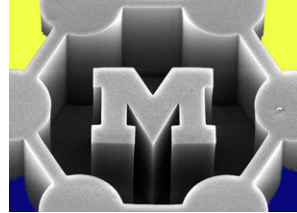
# Single nanotube radio!



Jensen et al., Nano Letters 7(11):3508-3511, 2007.

<http://www.physics.berkeley.edu/research/zettl/projects/nanoradio/radio.html>

# CNTs: modulus is chirality-dependent



$$E_{\text{armchair}} < E_{\text{zigzag}}$$

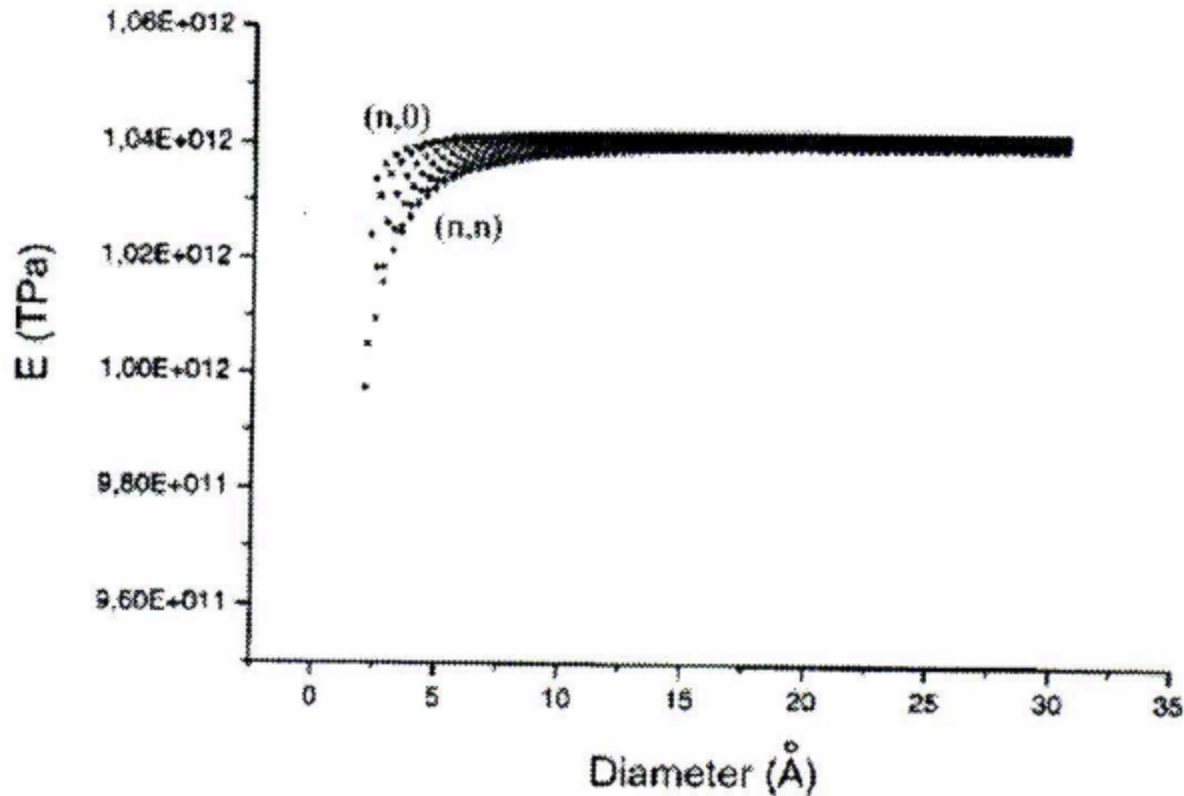
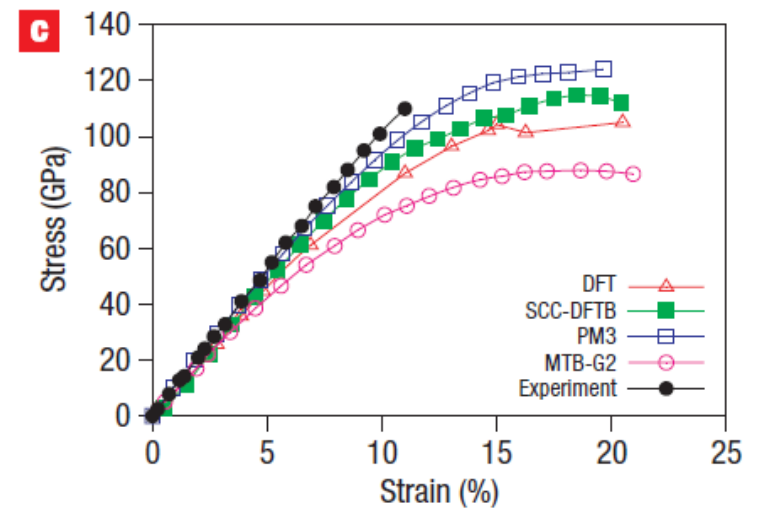
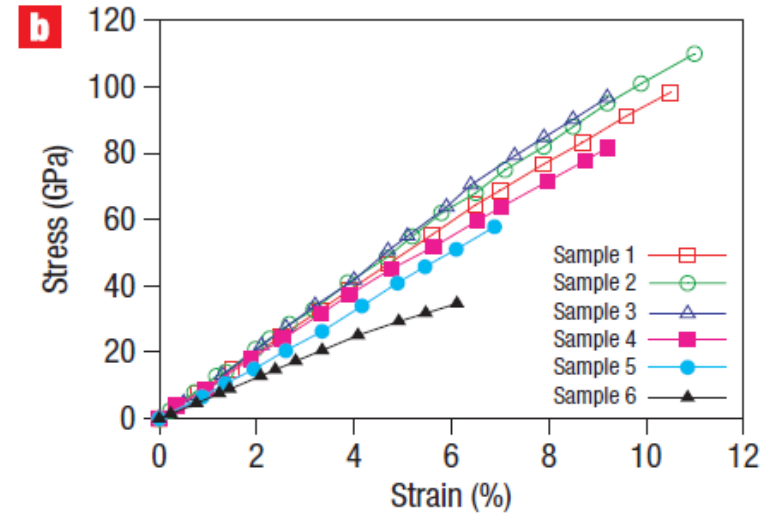
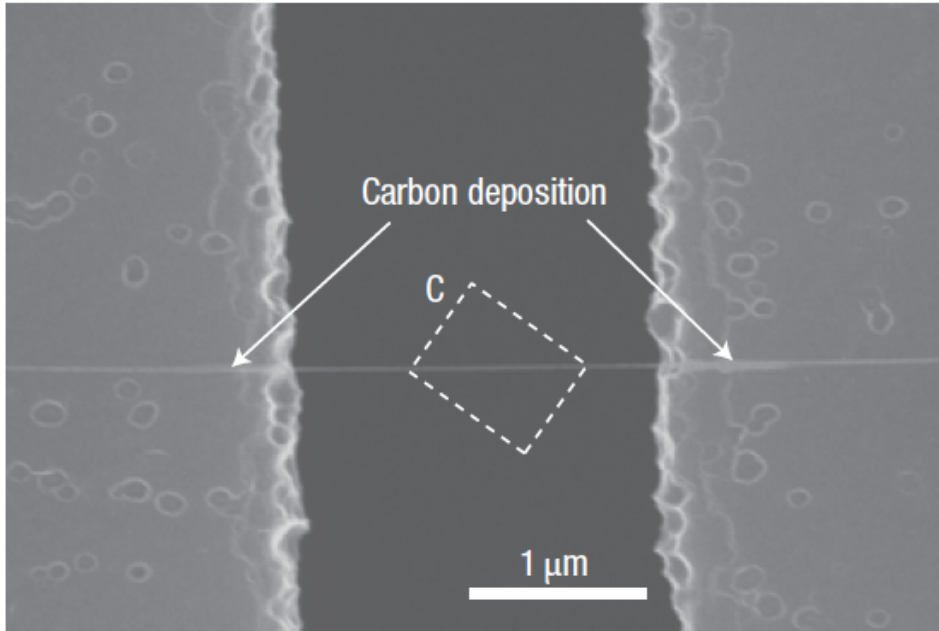
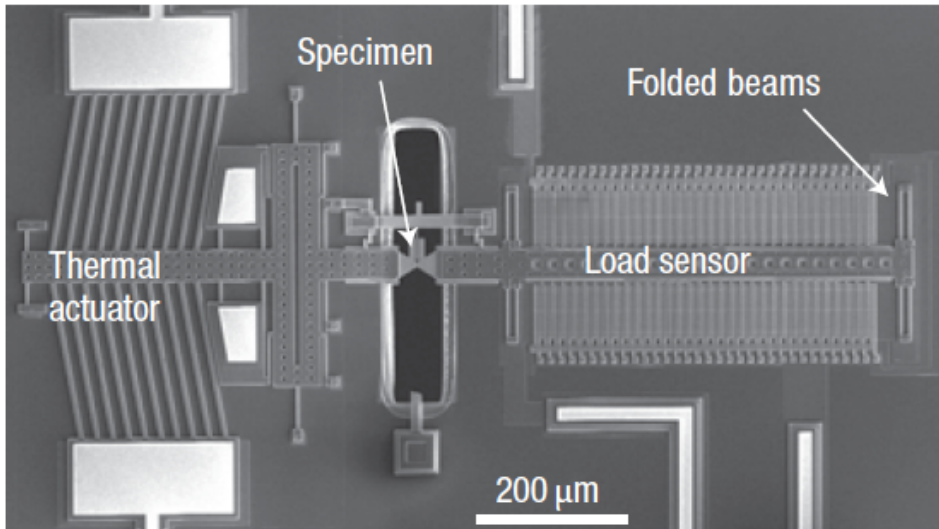
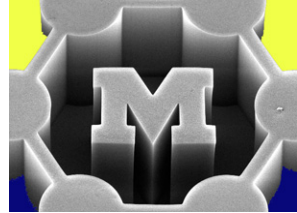


Fig. 7.8. Young's modulus as a function of the diameter for zigzag and armchair SWNTs. Tersoff-Brenner potential, fully-optimized cell,  $t = 0.34$  nm. By courtesy of Philippe Lambin (unpublished results)

# A small tensile tester



# Wall buckling gives low bending modulus

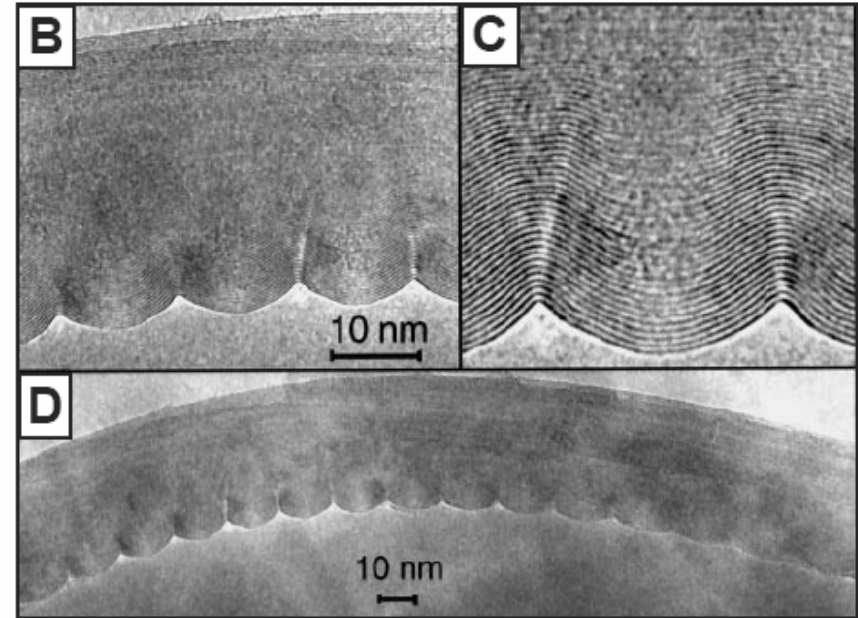
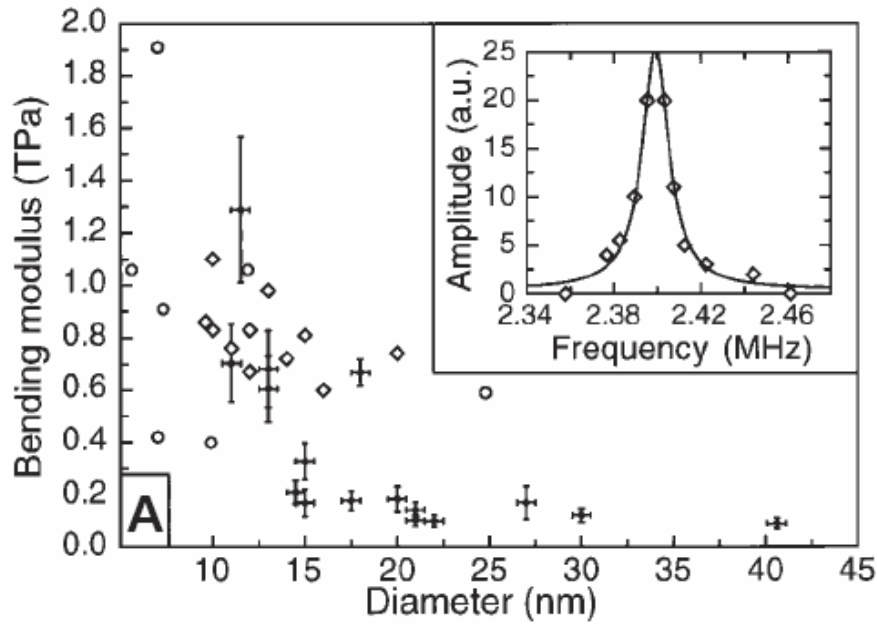
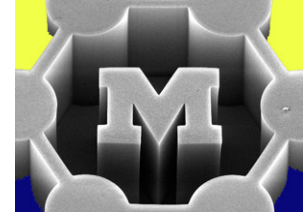
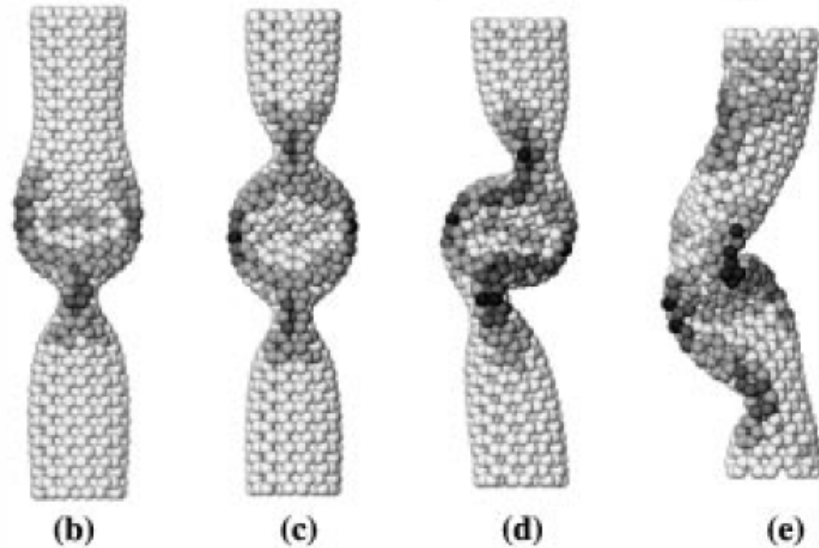
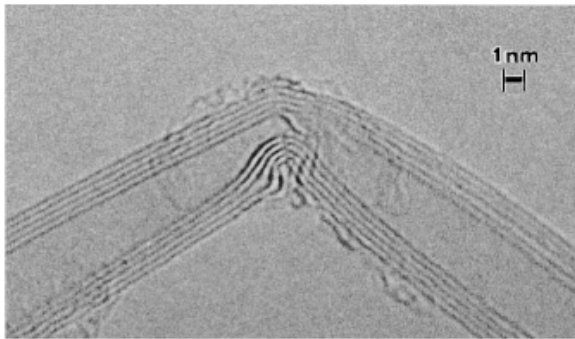
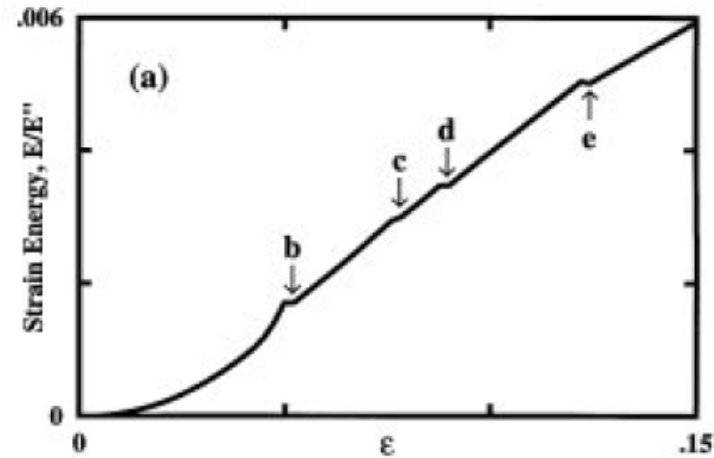
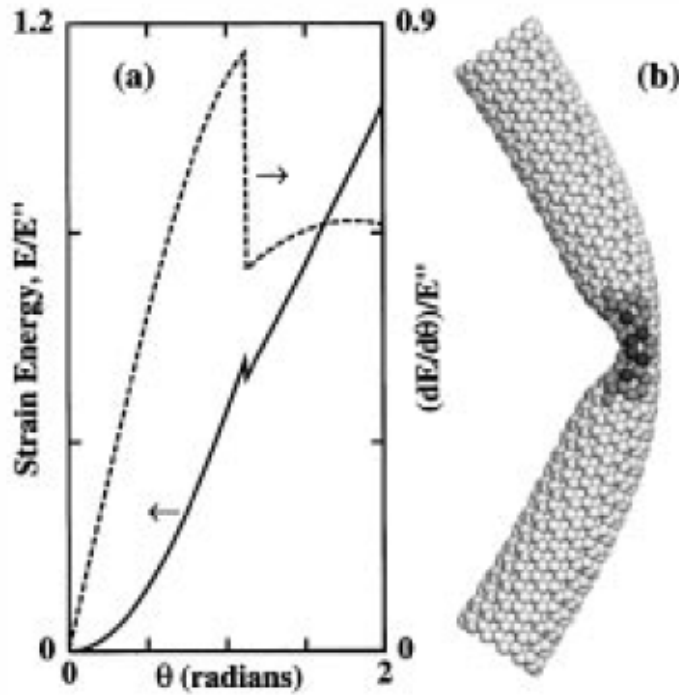
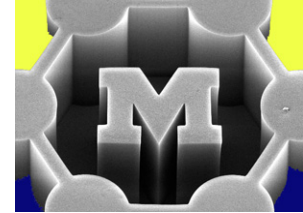


Fig. 3. Elastic properties of nanotubes. (A)  $E_b$  as a function of diameter: solid circles, present data; diamonds, data from (21); open circles, data from (12). [A further data point at  $D = 32.9$  nm and  $E_b = 1.26$  TPa from (16) is obscured by the inset.] Error bars indicate absolute error in  $L$  and  $D$ ; the error in the resonant frequency is negligible. The dramatic drop in  $E_b$  for  $D \approx 12$  nm is attributed to the onset of a wavelike distortion, which appears to be the energetically favorable bending mode for thicker nanotubes. There is no remarkable change in the Lorentzian line shape of

the resonance (inset) for tubes that have large or small moduli, although the low-modulus nanotubes appear to be more damped than the high-modulus tubes. (D) High-resolution TEM image of a bent nanotube (radius of curvature  $\approx 400$  nm), showing the characteristic wavelike distortion. (B and C) Magnified views of a portion of (D). The amplitude of the ripples increases continuously from the center of the tube to the outer layers of the inner arc of the bend. Note the absence of discontinuities in the interlayer spacing.

# CNTs kink like straws



Euler-type buckling in general case; hollow cylinder;  
shell buckling for short or large-diameter CNTs

Yakobson et al., Physical Review B 76(14), 1996.

Iijima et al., Journal of Chemical Physics 104:2089-92, 1996.

# Superplastic elongation of CNTs

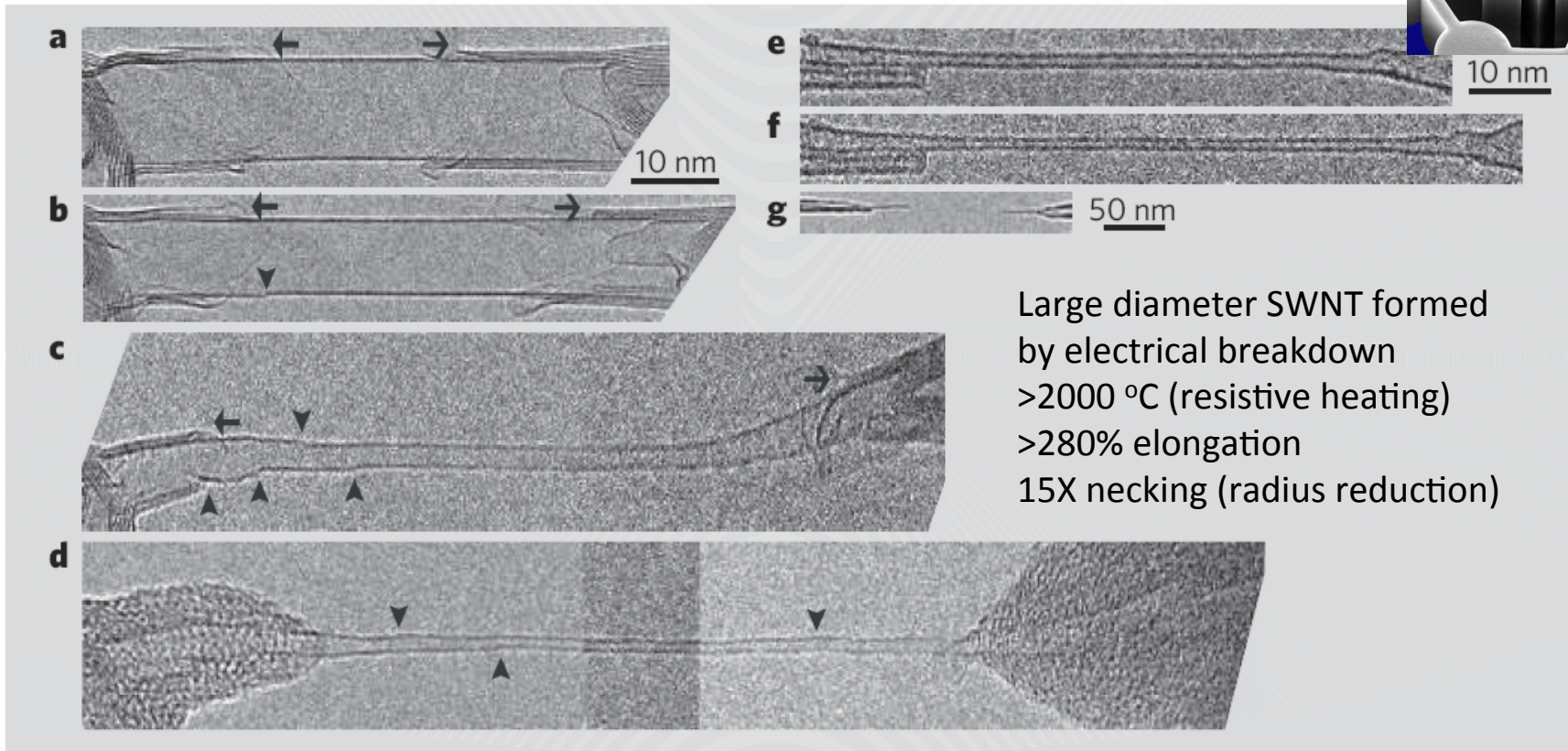
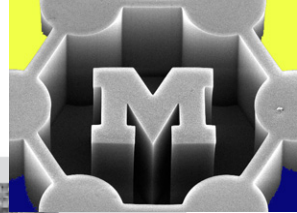
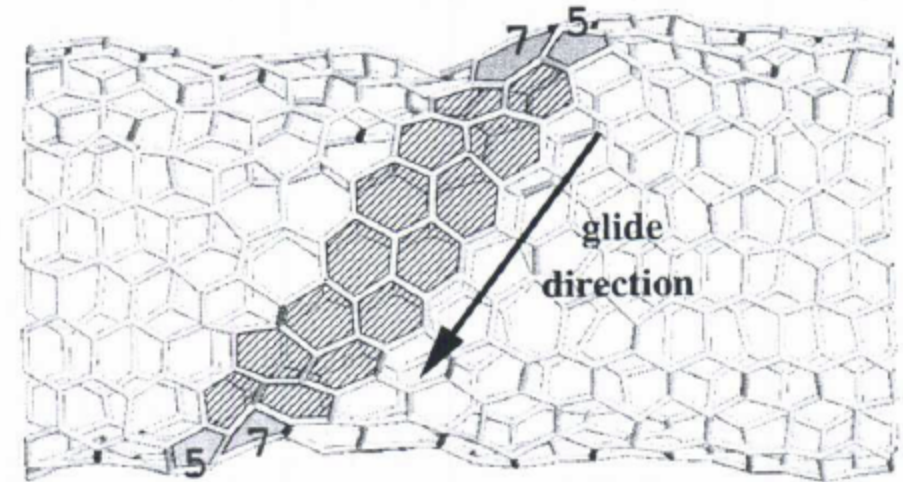
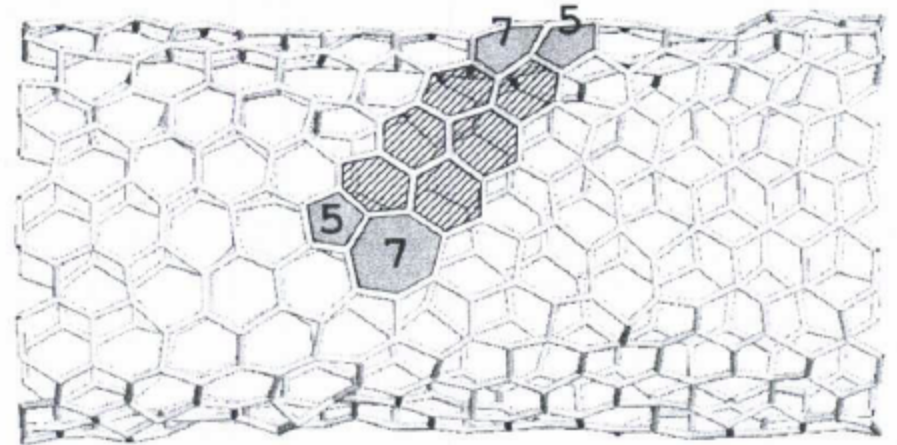
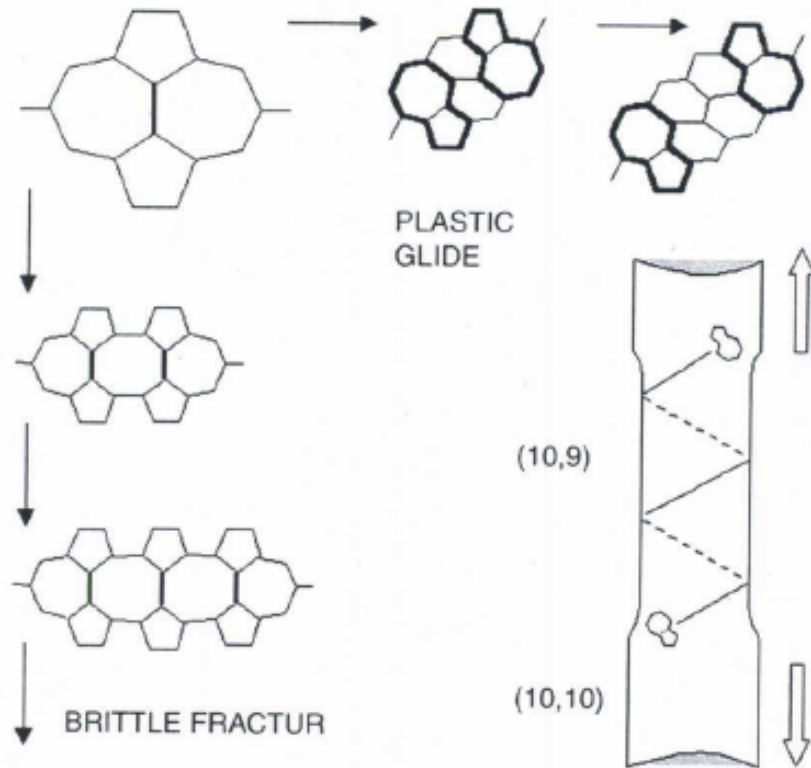
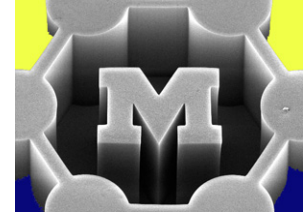
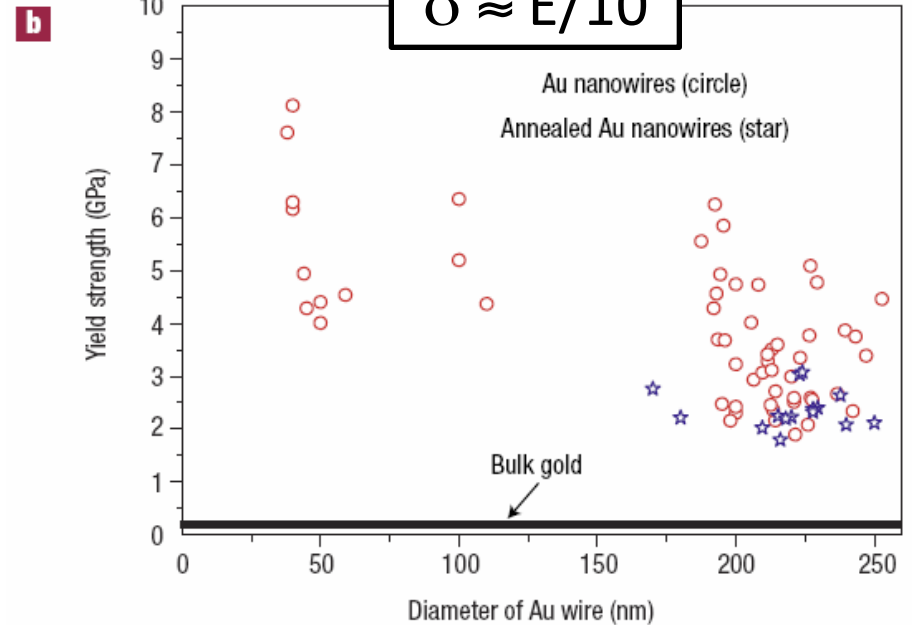
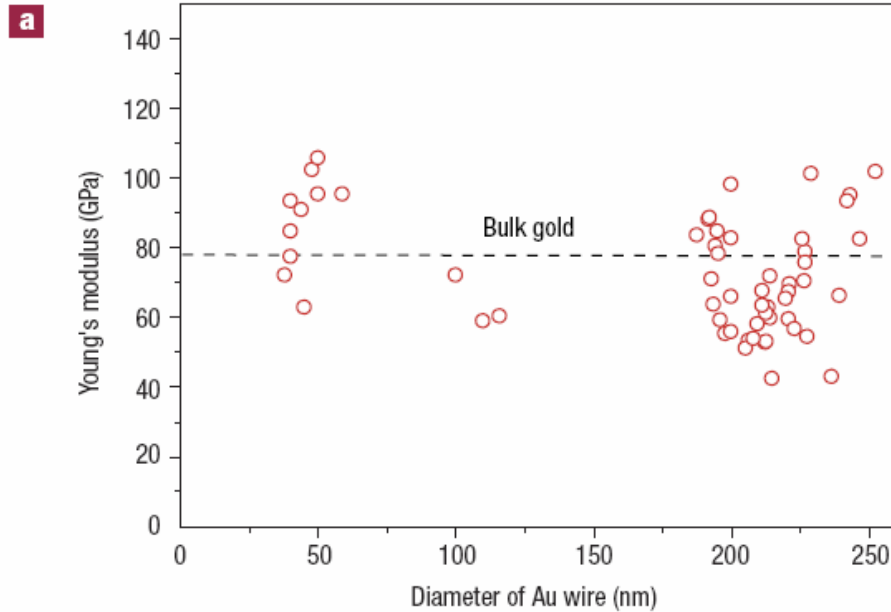
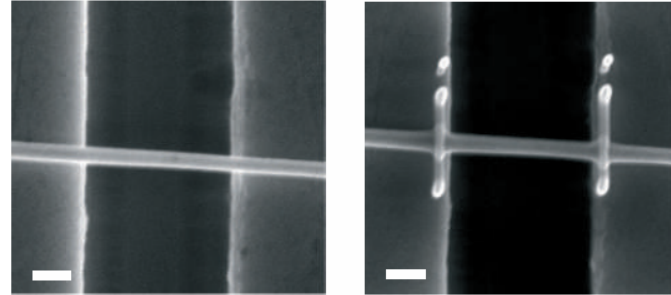
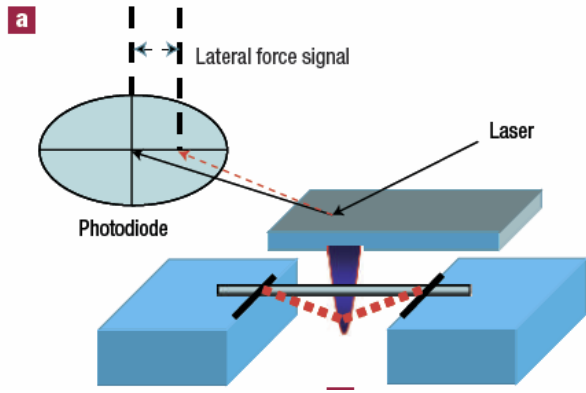


**Figure 1 | *In situ* tensile elongation of individual single-walled carbon nanotubes viewed in a high-resolution transmission electron microscope.** **a-d**, Tensile elongation of a single-walled carbon nanotube (SWCNT) under a constant bias of 2.3 V (images are all scaled to the same magnification). Arrowheads mark kinks; arrows indicate features at the ends of the nanotube that are almost unchanged during elongation. **e-g**, Tensile elongation of a SWCNT at room temperature without bias (images **e** and **f** are scaled to the same magnification). Initial length is 75 nm (**e**); length after elongation (**f**) and at the breaking point (**g**) is 84 nm; **g**, low-magnification image of the SWCNT breaking in the middle.

# Plastic glide of 5-7-7-5 defects



# Size-dependent observations for Au NWs



# At the nanoscale, we see distributions of strength values (here for WS<sub>2</sub> NTs)

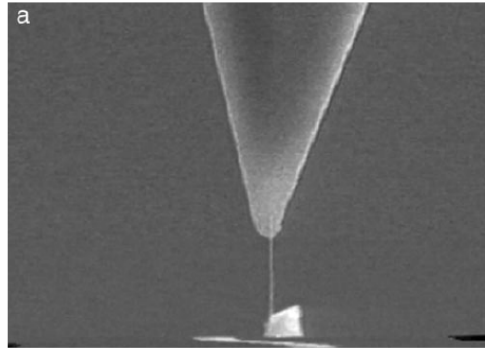
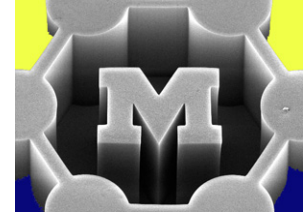


Table 1. The tensile strength results of WS<sub>2</sub> nanotube

Length, $\mu\text{m}$	Diameter, nm	Force, N	Strength, GPa	Strain, %	E, GPa
2.17	20	5.87E-7	15.10	—	—
2.95	30	5.71E-7	9.77	8.30	119.9
2.03	20	3.37E-7	8.66	8.70	150.4
2	34	1.31E-7	3.75	—	—
1.55	25	7.83E-7	16.09	—	—
4.6	25	5.87E-7	15.07	5.03	218.0
0.85	30	7.78E-7	13.32	10.08	81.6
2.4	36	1.14E-6	16.27	11.60	244.0
2.09	19	2.49E-7	6.74	6.90	102.2
1.81	18	5.55E-7	15.8	14.00	109.3
1	11	2.91E-7	13.58	12.70	87.6
1.09	21	3.45E-7	8.42	—	—
1.97	20	5.83E-7	14.97	11.10	255.3
1.7	20	3.0E-7	7.70	—	—
0.77	20	4.3E-7	11.05	—	—
2.8	20	4.87E-7	12.50	7.75	151.4

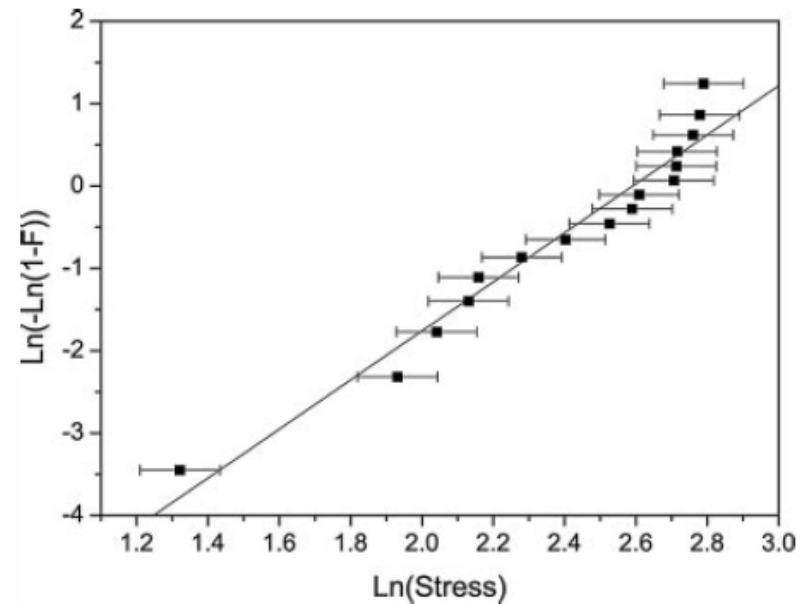
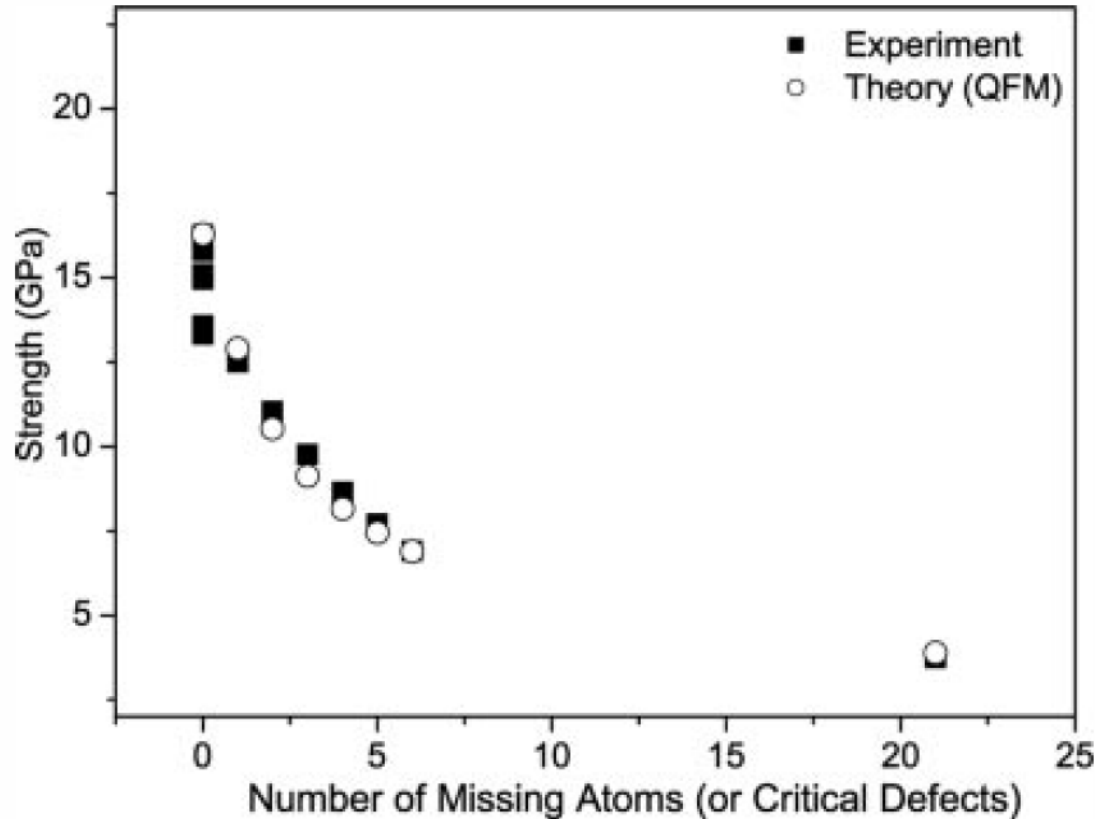
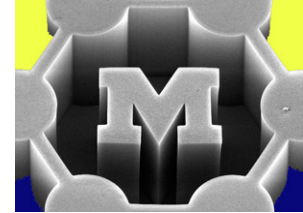


Fig. 4. Weibull plot:  $\text{Ln}(-\text{Ln}(1 - F))$ , where  $F$  is the probability of failure at a given stress vs.  $\text{Ln}(\text{Stress})$ . The probability of failure can be described by the Weibull model if the plot is linear.

and strength can depend on the size of the initial “critical” defect (here in  $WS_2$  NWs)



$$\sigma_f(n) = \sigma_c \left( 1 + \frac{\rho}{2a} \right)^{1/2} (1 + n)^{-1/2},$$

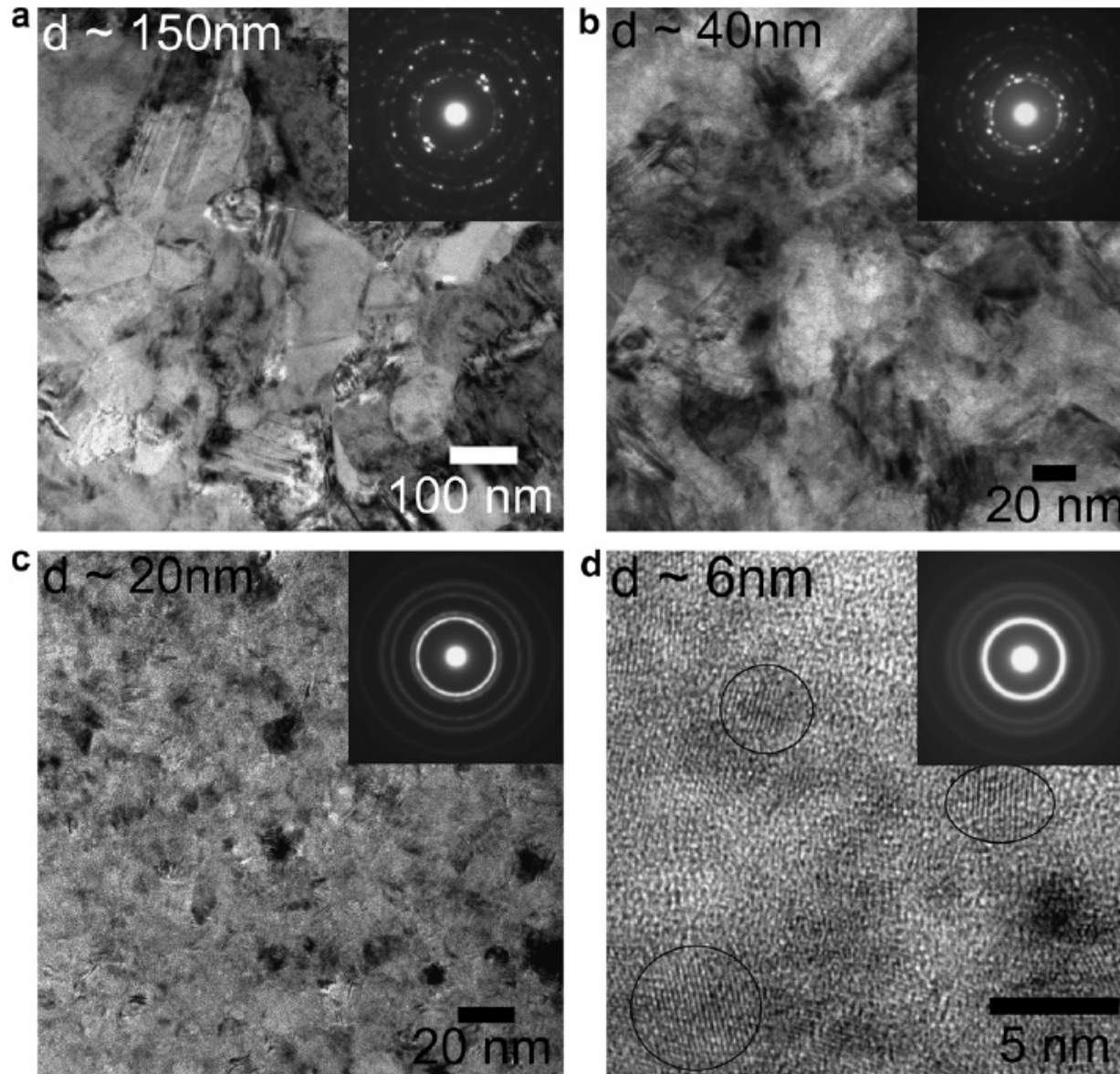
$n$  = number of missing atoms

$\sigma_c$  = ideal strength

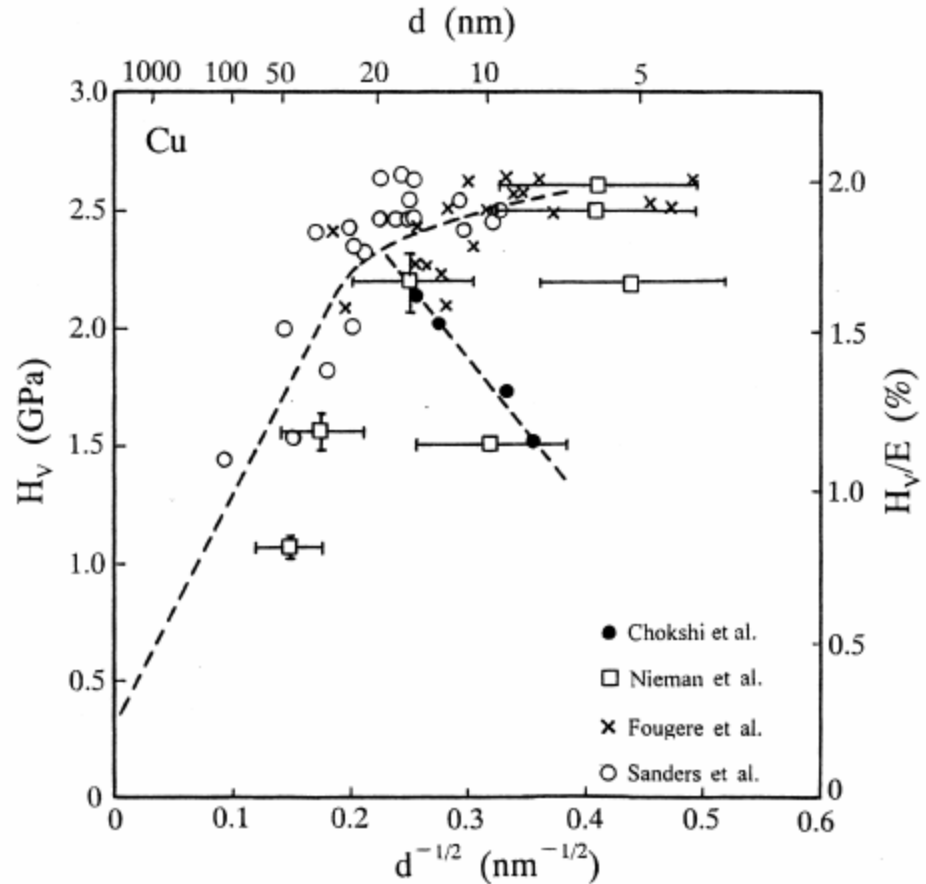
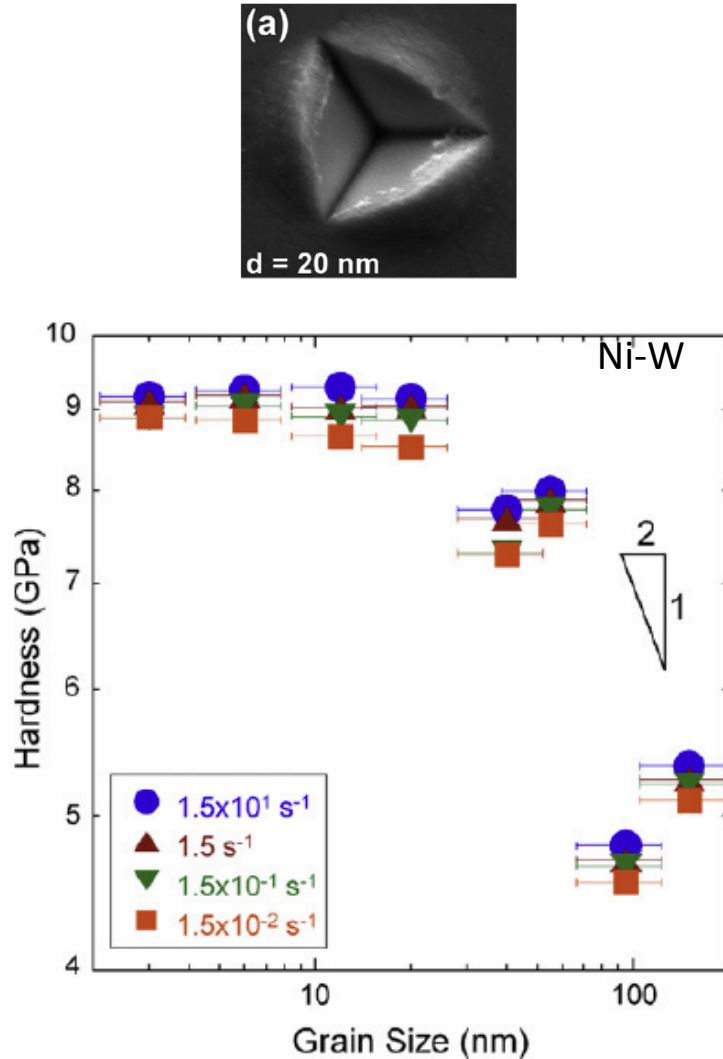
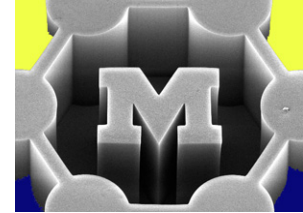
$\rho$  = radius of rupture

$a$  = lattice parameter

# Bulk nanocrystalline materials (Ni-W)



# Nanostrengthening bulk materials: the Hall-Petch relation



Trelewicz and Schuh, *Acta Materialia* 55:5948-5958, 2007.

Takeuchi, *Scripta Materialia* 44:1483-1487, 2001.

# Strategies for boundary engineering

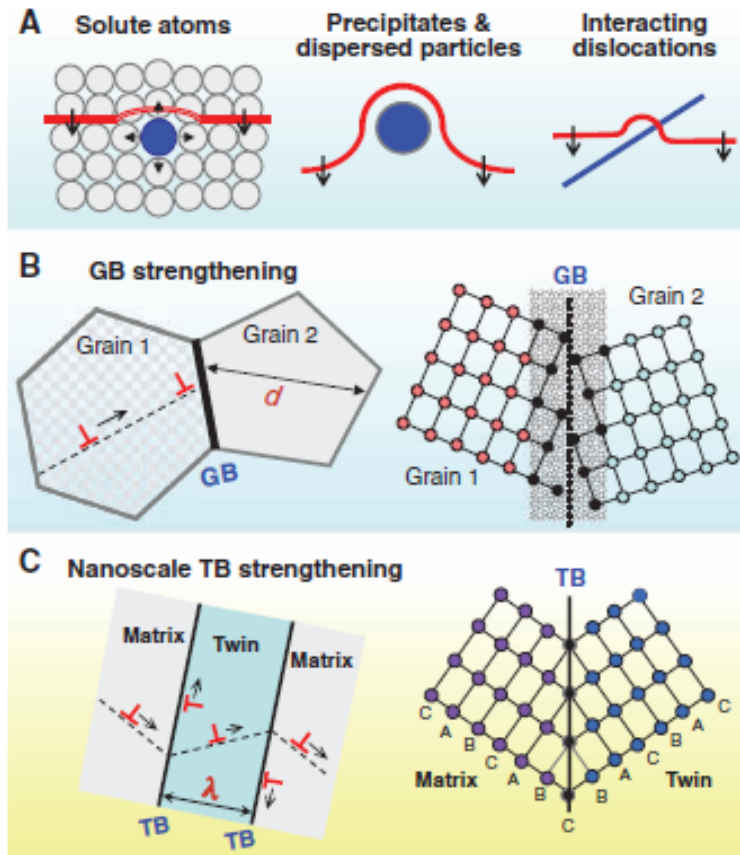
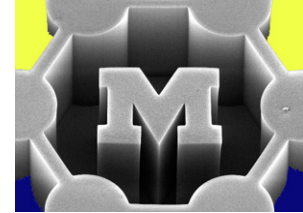


**Fig. 1.** Schematic illustration of examples of structural modifications for strengthening metals and alloys. Commonly used strengthening methods include (A) strengthening via solid solution, whereby solute atoms strain the matrix to impede the motion of a dislocation (red line) through the lattice; via precipitates or dispersed particles that interact with mobile dislocations, leading to overall strengthening of the material; or via elastic interactions between intersecting dislocations (blue and red lines), as well as geometry changes and subsequent obstructions to slip (as, for example, through the formation of sessile dislocation segments) associated with such encounters. GB strengthening (B) is another commonly used method in which dislocation (red  $\perp$  symbol) motion is blocked by GB (whose incoherent structure is schematically shown on the right) so that a dislocation pile-up is formed. A higher stress is needed to deform a

polycrystalline metal with a smaller grain size  $d$  (more GBs). (C) Nanoscale TB strengthening is based on dislocation-TB interactions from which mobile and/or sessile dislocations could be generated, either in neighboring domains (twin or matrix) or at TBs. Gliding of dislocations along TBs is feasible because of its coherent structure [the right panel in (C) denotes a  $\Sigma 3$  TB]. Higher strength and higher ductility are achieved with a smaller twin thickness  $\lambda$  in the nanometer scale.

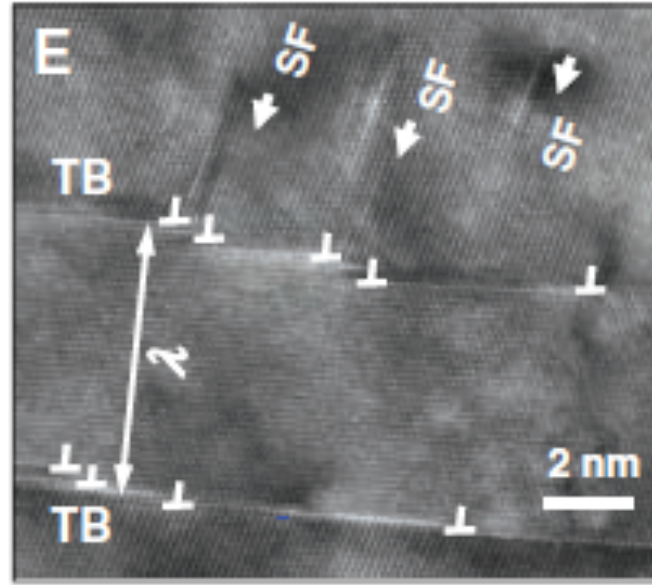
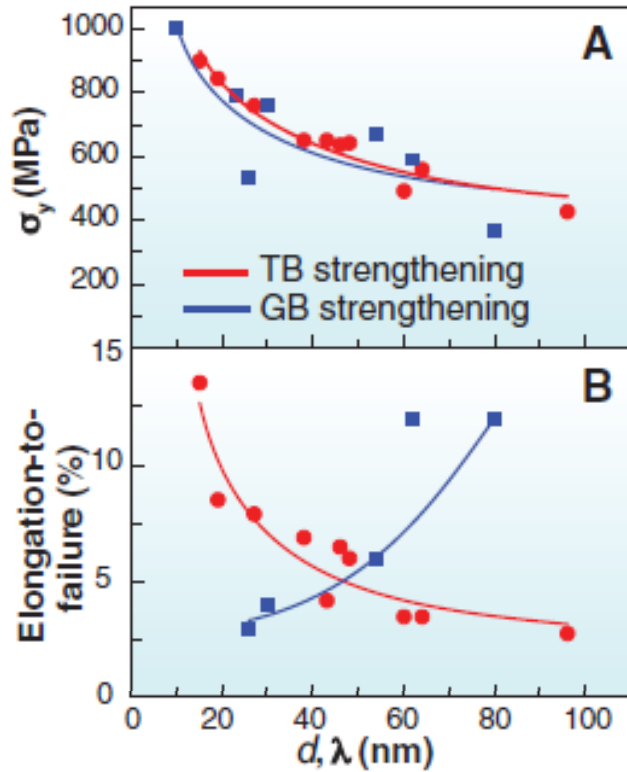
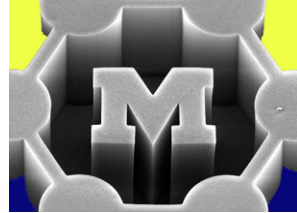
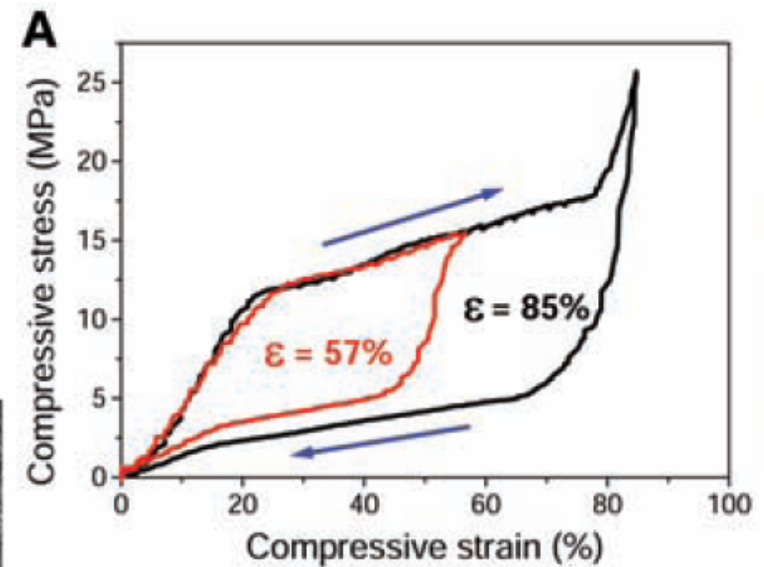
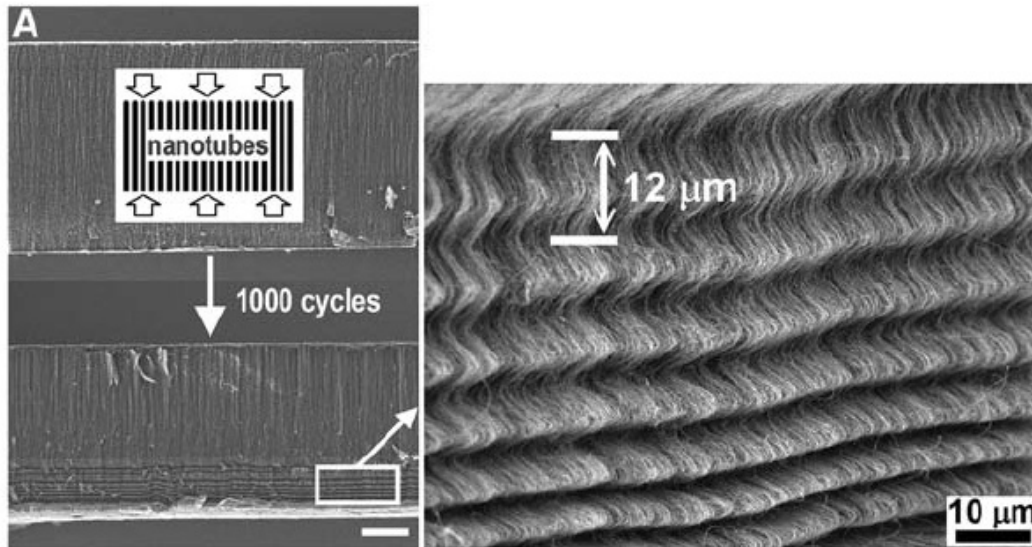
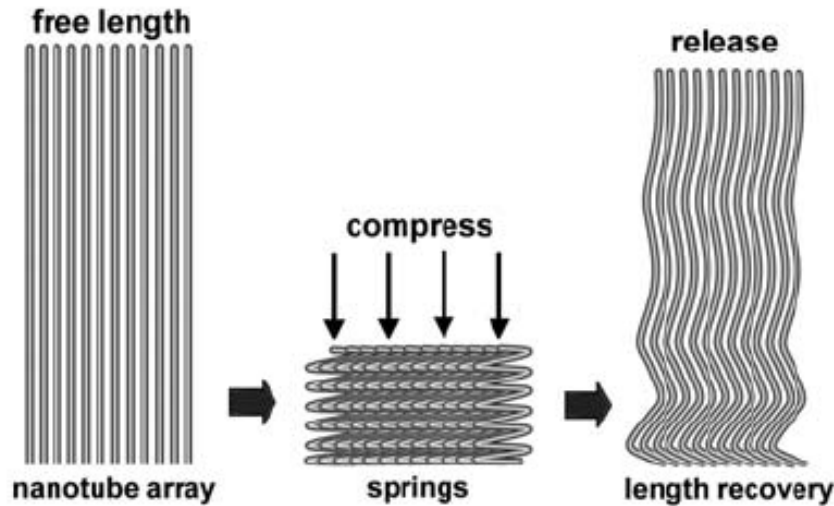
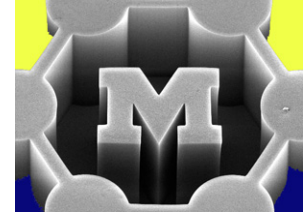


**Fig. 2.** Experimental results comparing the effectiveness of TBs in influencing mechanical properties with that of GBs for pure Cu. The characteristic structural dimensions used as a basis for comparison are  $\lambda$  and  $d$ . **(A)** Strength/hardness ( $\sigma_y$ ), **(B)** elongation to failure, and **(C)** rate sensitivity of flow stress characterized by the parameter  $m$ . Error bars indicate  $\pm$ SD from the mean of three samples. **(D)** Schematic illustration of the known effect of grain size  $d$  on stress-life fatigue response (left and top axes) characterized by the stress amplitude ( $\sigma_{amp}$ ) and the number of stress reversals to failure ( $2N_f$ ). Resistance to subcritical fatigue fracture characterized by the rate of fatigue crack growth ( $da/dN$ ) versus the stress intensity factor range ( $\Delta K$ ) is plotted on a log-log scale on the bottom and right axes. Here, grain refinement generally leads to higher crack growth rates in the low- and mid- $\Delta K$  range. Similar behavior is anticipated for refinement of nanotwin thickness  $\lambda$ . **(E)** HRTEM image of the interaction of dislocations with nano TBs in pure Cu that had previously been deformed in tension. Arrows indicate the stacking faults (SF). Image reproduced with permission from (19).

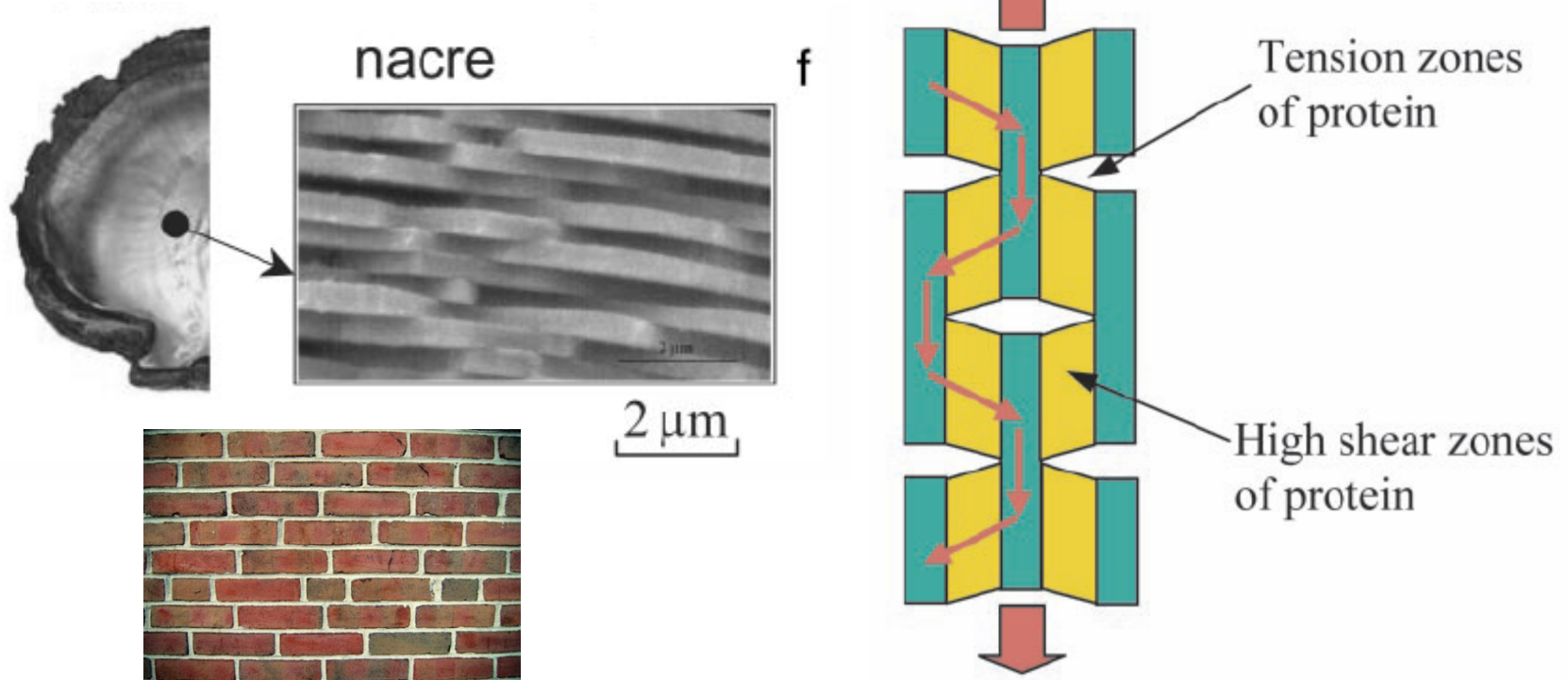
# Collective properties: CNT foams



# Nacre (mother of pearl): distributed flaw tolerance



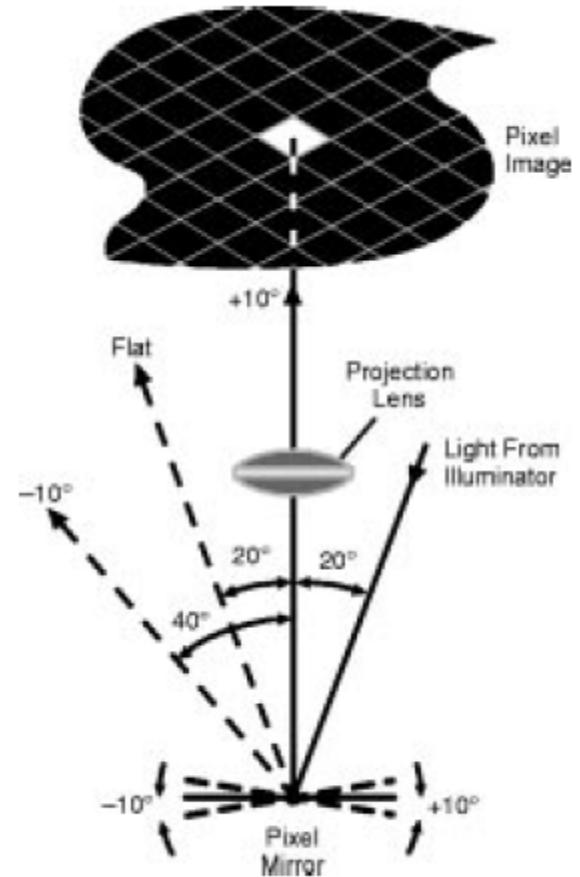
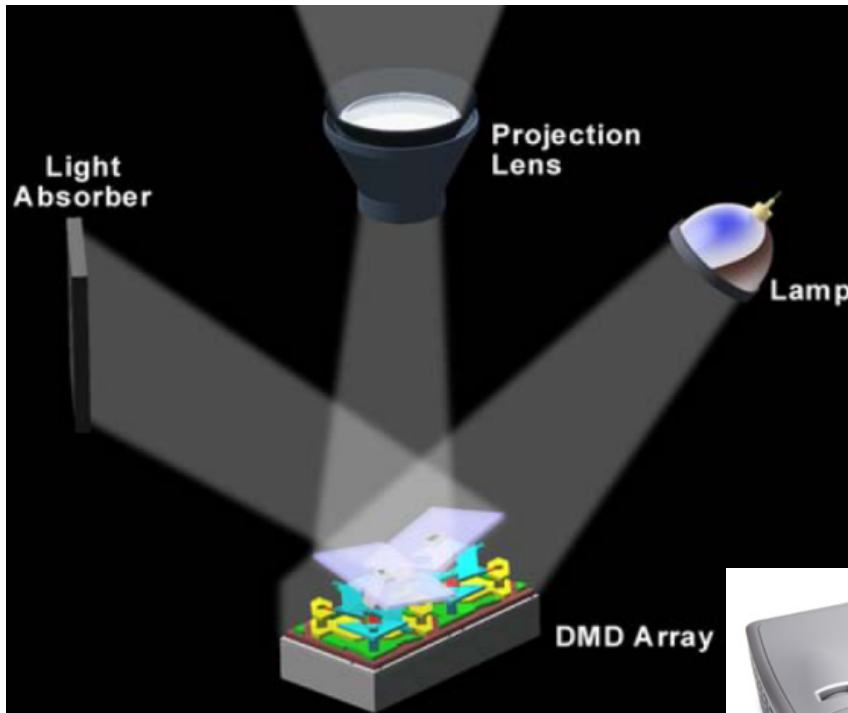
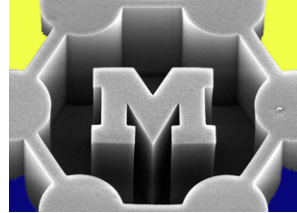
- Hexagonal platelets of aragonite (a form of calcium carbonate) 10-20  $\mu\text{m}$  wide and 0.5  $\mu\text{m}$  thick, arranged in a continuous parallel lamina, separated by sheets of elastic biopolymers (such as chitin, lustrin and silk-like proteins)



- Many other examples in nature (e.g., skeletons, snail shells)

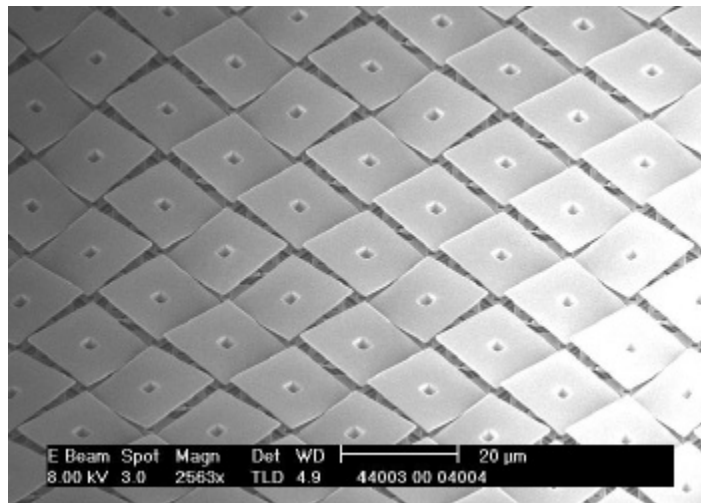
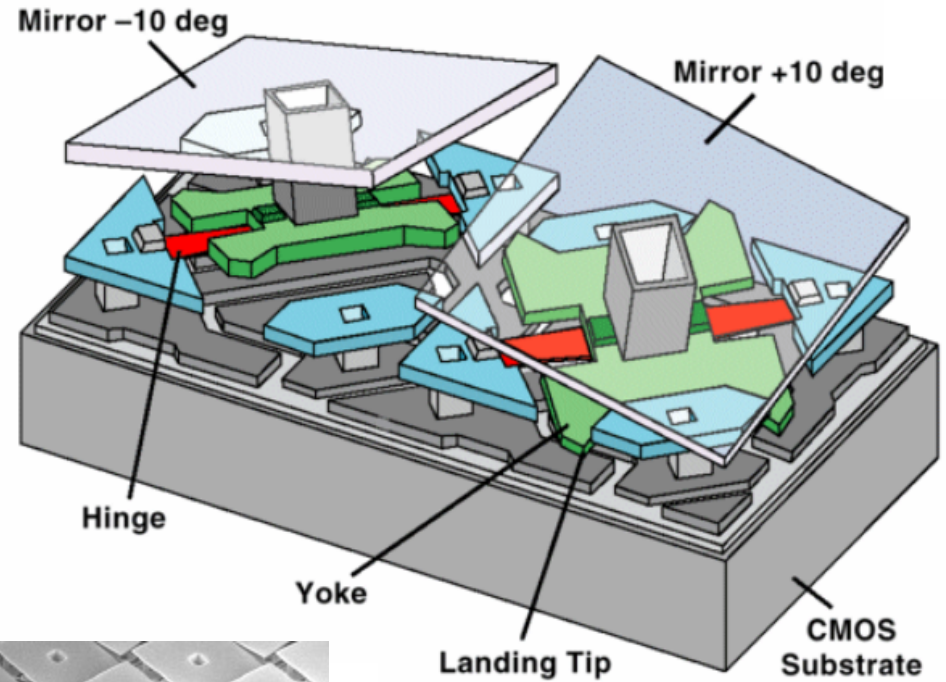
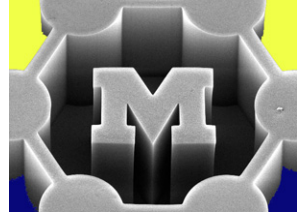
# DMD projector

- Projection display based on changing the angle of micromirrors (electrostatic actuation)
- Invented 1987; shipped 1996.
- Support cantilevers are single-crystal Ni

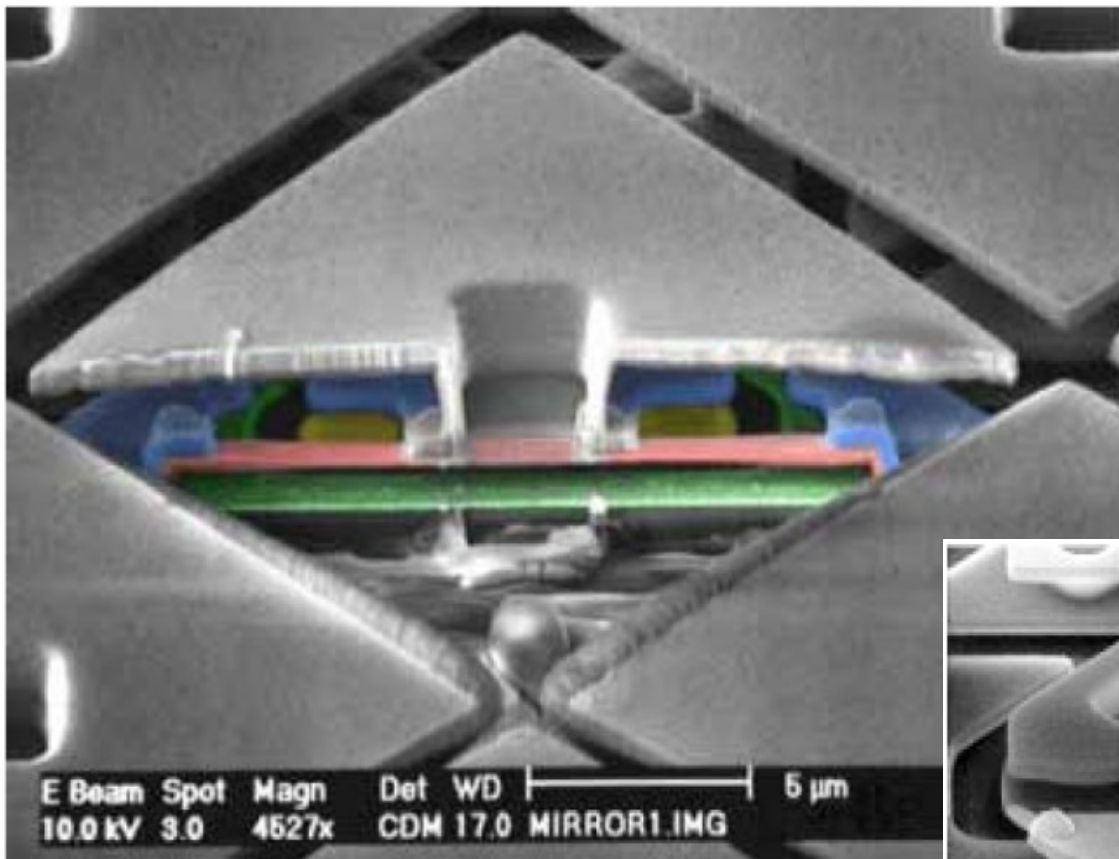
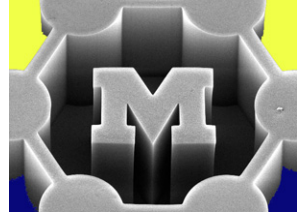


# DMD structure

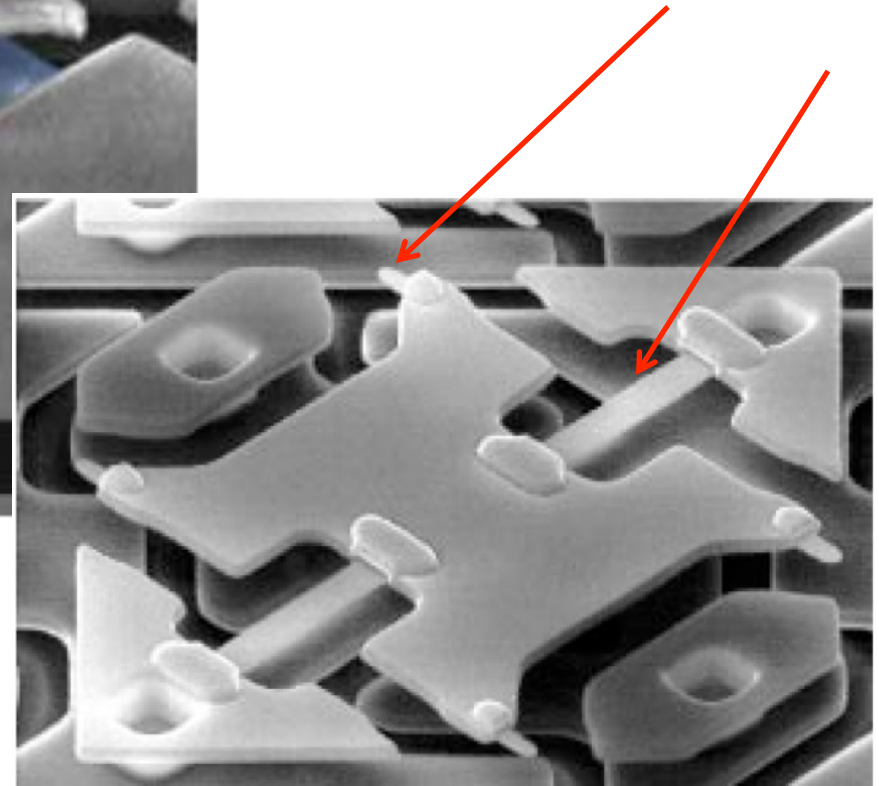
- 4 x 4 micron mirror
- Hinge (flexure)
- Yoke
- Connecting posts
- Electrostatic actuator
- CMOS control / addressing circuit (memory array)
- Moving parts are aluminum



E Beam	Spot	Magn	Det	WD	20 $\mu$ m
8.00 kV	3.0	2563x	TLD 4.9	44003 00 04004	



- The hinges are 60 nm thick by 600 nm wide
- The hinges are flexed  $\pm 10^\circ$
- For a bulk hinge, torsion will result in plastic deformation after only a few cycles



# Hinge fatigue and “memory”



- NO fatigue failures
  - $3 \times 10^{12}$  device cycles = 120 years life at 1000 hours per year
  - 500,000 mirrors per device  $\rightarrow$   $14 \times 10^{18}$  individual mirror cycles without a single hinge fatigue failure!

